BALBI EQUATION

FUNDAMENTAL CONCEPTS AND PRINCIPLES

A NEW EXPLICIT, NON-ITERATIVE, AND UNIFIED MODEL FOR DISTRIBUTED PRESSURE DROP CALCULATIONS IN DUCTS

Author: **VINÍCIUS CABRAL BALBI**[1]

ASHRAE MEMBER – HVAC DESIGNER TECHNICIAN

July - 2026

[1] Technical review by Mechanical Engineers PEDRO HENRIQUE NEIVA DE PONTES and JUAN DE CARVALHO SILVA. The author expresses his gratitude for their critical reading and suggestions.

The author also thanks to DANIEL FELIPE LINHARES DOS SANTOS SILVA for all his support and trust.

ABSTRACT

This paper presents the **Balbi Equation**, a phenomenological and semi-empirical formulation for estimating distributed pressure drop in circular ducts. Rather than replacing established methods, the proposed approach offers an alternative physical interpretation of flow resistance while remaining consistent with classical fluid mechanics and established engineering practice. The model combines analytical development with experimental calibration through five fundamental relationships: (1) the viscous wavelength, $\lambda = \frac{\nu}{v_m} \cdot k_{Balbi}$, representing an effective characteristic length associated with viscous momentum diffusion; (2) a unified exponential velocity profile, $u(r) = v_{max}\left(1 - e^{-((R-r)/\lambda)^{\alpha}}\right)$, applicable to laminar, transitional, and turbulent regimes; (3) a continuous flow-regime function, $\alpha(Re) = 1 + \frac{1}{1+(Re/2800)^4}$, providing a smooth transition between flow regimes; (4) a pressure-drop expression, $\frac{\Delta P}{L} = \frac{2\mu v_{max}\alpha}{R\lambda} \cdot \frac{1}{1000}$, derived directly from the proposed velocity profile; and (5) a calibration relationship, $k_{Balbi} = C_{base} Re^{0.25} \left(\frac{\varepsilon}{D_h}\right)^{0.1}$, which relates the characteristic viscous scale to wall roughness and flow conditions.

The formulation was validated against two independent experimental datasets. For corrugated flexible ducts (Dai et al., 2021), it achieved a precise prediction error of +4.5%, whereas the Colebrook–White equation underestimated the pressure drop by −14.8%. In gas–liquid–solid three-phase flows (Al-Hadhrami et al., 2014), the phenomenological framework proved highly adaptable beyond conventional HVAC domains. For standard galvanized steel ducts in HVAC applications (C_{base} = 0.042), the model yields consistently stable, conservative margins (ranging from +21% to +27%) relative to the Colebrook–White equation.

Operating with a constant-time computational complexity of $\mathcal{O}(1)$, the Balbi Equation eliminates iterative processes, offering a physically motivated and computationally efficient alternative for spreadsheet and software implementation in engineering design.

$$\lambda = \frac{\nu}{v_m} \cdot k_{Balbi}$$

$$k_{Balbi} = C_{base} Re^{0.25} \left(\frac{\varepsilon}{D_h}\right)^{0.1}$$

$$u(r) = v_{max}\left(1 - e^{-((R-r)/\lambda)^{\alpha}}\right)$$

$$\alpha(Re) = 1 + \frac{1}{1 + (Re/2800)^4}$$

$$\frac{\Delta P}{L} = \frac{2\mu v_{max}\alpha}{R\lambda} \cdot \frac{1}{1000}$$

***Keywords**: Pressure drop; duct design; Balbi equation; explicit method; HVAC; viscous wavelength; Colebrook-White; non-iterative.*

TABLE OF CONTENTS

1. INTRODUCTION

Internal flow in circular ducts is one of the most consolidated pillars of fluid mechanics. Since the pioneering experiments of Hagen, Poiseuille, Darcy, Reynolds, Blasius, Nikuradse, and Colebrook, distributed pressure drop has been modeled as the macroscopic manifestation of the complex interaction between inertial forces, molecular viscosity, and the geometric roughness of the duct walls. Over the last century, this conceptual framework gave rise to the classical Darcy-Weisbach formulation and the semi-empirical correlations for determining the friction factor—fundamental and indispensable tools for the design of modern hydraulic, thermal, and HVAC systems.

However, despite the mathematical robustness and practical precision of these traditional formulations, the transition between flow regimes and the determination of friction in intermediate zones are still frequently treated through segmented approximations, discontinuous correction factors, and iterative computational processes. From this purely mathematical perspective, fluid behavior ends up being represented by the concatenation of distinct models for each operational range, which may distance the analysis from a continuous physical interpretation of dissipative mechanisms.

The motivation for this work arises from this conceptual gap. We propose herein an alternative analytical and phenomenological formulation for calculating distributed pressure drop, termed the Balbi Equation. Based on the concept of the viscous wavelength (λ), the model introduces a spatial scale that continuously describes the transition between laminar, transitional, and turbulent regimes without resorting to discontinuities or conditional logic in the modeling. Initially calibrated for applications in HVAC, industrial ventilation, and technical ducts, the mathematical structure of the formulation aims to provide a complementary and explicitly direct tool for engineering, aligned with the historical foundations consolidated by classical literature.

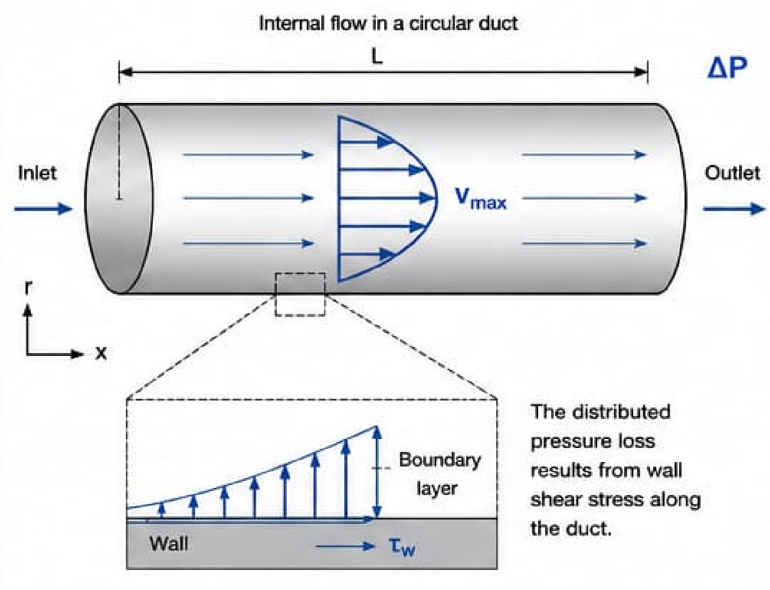

Figure 1 – Schematic representation of internal flow in a circular duct, highlighting the development of the velocity profile and the origin of distributed pressure drop due to wall shear

2. SCIENTIFIC POSITIONING AND PHENOMENOLOGICAL NATURE OF THE MODEL

The Balbi Equation is a phenomenological and semi-empirical formulation. This implies that its central objective is not to replace the fundamental principles of fluid mechanics, nor to compete with general Navier-Stokes equations or advanced computational simulation methods—such as Computational Fluid Dynamics (CFD), Large Eddy Simulation (LES), or Direct Numerical Simulation (DNS). The validation of a new conceptual proposal requires rigorously delimiting its nature, applicability, and limitations. Turbulence remains one of the most complex open problems in classical physics, and the approach proposed herein operates at the macroscopic scale of applied engineering.

The originality of the model lies in reorganizing the dissipation phenomenon based on the dynamic spatial relationship between the fluid and the conduit. All distributed pressure drop arises, essentially, from the transfer of momentum by shear. From this viewpoint, we adopt the physical hypothesis that viscosity establishes an effective depth for the propagation of the braking effect imposed by the wall upon the flow, quantified by the viscous wavelength (λ). While in the laminar regime this dissipative zone occupies virtually the entire cross-section of the duct, the increase in the Reynolds number and the resulting turbulent intensity progressively compress this scale toward the wall, concentrating the velocity gradient in a narrow peripheral region.

To mathematically translate this spatial mechanism and ensure model closure, we introduce the flow-regime function and the coupling coefficient. This coefficient is semi-empirical in nature and is determined from the analytical equivalence between the wall shear stress predicted by the proposed exponential velocity profile and the experimental correlations widely consolidated in technical literature.

Admitted as a proposal in constant evolution, the model does not claim absolute universality. The Balbi Equation should be interpreted as a complementary conceptual framework. Its practical utility lies in the elimination of iterative routines and the possibility of representing pressure drop through a continuous and spatially motivated physical interpretation.

3. FUNDAMENTALS OF THE VISCOUS WAVELENGTH λ

In classical internal flow models, distributed pressure drop is traditionally interpreted as a consequence of energy dissipation caused by friction between the fluid and the duct wall. However, from a phenomenological perspective, this interaction can be reinterpreted in a spatial and continuous manner.

Every wall imposes resistance to fluid motion. This resistance does not act instantaneously upon the entire flow but propagates its influence progressively through adjacent fluid layers via viscous shear. Thus, dissipation can be understood as a process of gradual transmission of the deceleration imposed by the wall to the rest of the fluid.

Under this interpretation, the wall acts as the central dissipative element of internal flow, establishing an effective reach of influence over the fluid mass in motion.

Balbi Equation proposes to represent this dissipative reach through the viscous wavelength λ:

$$\lambda = \frac{\nu}{v_m} \cdot k_{Balbi}$$

Where:

- ν is the fluid kinematic viscosity [m²/s];
- v_m is the mean flow velocity [m/s];
- k_{Balbi} is the viscous coupling coefficient (dimensionless), the unified formulation of which will be detailed in Section 6.

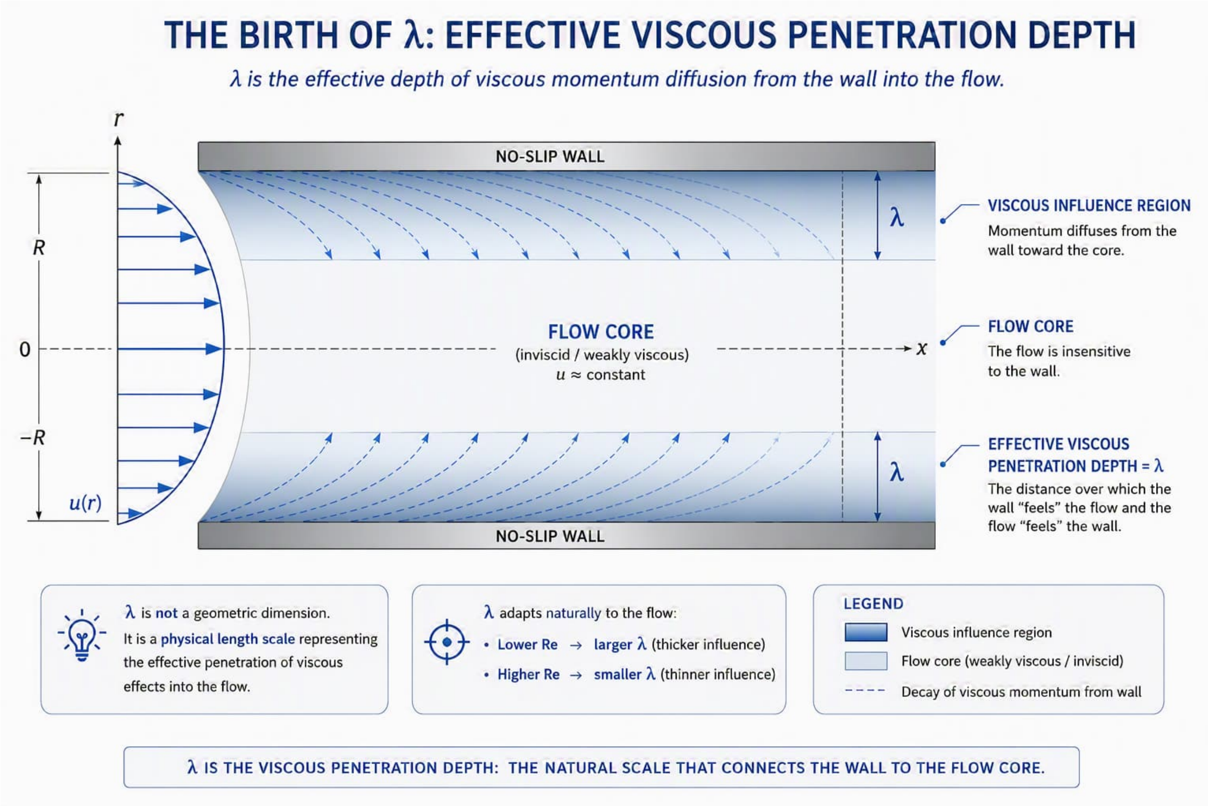

Figure 2 - Conceptual representation of the viscous penetration depth (λ). The parameter λ denotes the effective dissipative length scale through which wall-induced viscous effects extend into the flow, linking wall friction to the development of the velocity profile.

3.1 Immediate Physical Interpretation

Situation	**Effect on λ**	**Physical Meaning**
ν increases (more viscous fluid)	λ increases	The wall extends its "braking" further into the duct
v_m increases (faster flow)	λ decreases	The boundary sublayer is compressed; the velocity gradient at the wall becomes more severe
$k_{Balbi} > 1$	$\lambda > \nu / v_m$	The wall brakes further away (laminar regime or high roughness)
$k_{Balbi} < 1$	$\lambda < \nu / v_m$	Compressed boundary sublayer (high-speed turbulent regime)

Table 1 - Phenomenological interpretation applied to the model

3.2 The natural viscous length scale

Classical physics provides us with a natural viscous length scale:

$$\lambda_{ideal} = \frac{\nu}{v_m}$$

If the duct were perfectly smooth and the flow perfectly laminar, this would be the boundary layer thickness. In the real world, however, the duct surface possesses roughness, corrugations, joints, and imperfections. Turbulence also compresses or expands the boundary sublayer.

The coefficient k_{Balbi} is the coupling factor that connects this idealized scale to the real-world scale:

$$\lambda = \lambda_{ideal} \cdot k_{Balbi}$$

3.2.1 Physical limits of the viscous scale

For the model to be physically acceptable, strict limits must be respected:

Lower limit: The fluid at the wall is always "stuck" (no-slip condition). The viscous scale cannot be zero, which implies $k_{Balbi} > 0$.

Upper limit: The wall cannot brake the fluid beyond the geometric center of the duct (radius R), which imposes $\lambda \leq R$.

The quantitative treatment of these limits will be resumed in Section 6, following the unified formulation of k_{Balbi}.

4. MODELING THE TRANSITION BETWEEN FLOW REGIMES

The phenomenological interpretation proposed by the Balbi Equation naturally leads to the necessity of mathematically representing the continuous transition between different flow regimes.

In classical models, laminar and turbulent regimes are often addressed through distinct formulations, associated with different experimental correlations and friction factors. Although such approaches are extremely effective in practical applications, the shift between regimes generally occurs through segmented mathematical transitions, involving abrupt changes in the closure relationships utilized in these models.

From the phenomenological perspective adopted in this work, however, the transition between regimes is not interpreted as an instantaneous physical rupture, but as a progressive reorganization of the interaction between fluid inertia and the dissipative reach imposed by the wall.

As the Reynolds number increases, the viscous wavelength (λ) tends to decrease relative to the duct's geometric scale. This means that the spatial influence of the wall becomes progressively more concentrated near the peripheral region of the flow, while the central region becomes predominantly dominated by inertial effects.

This gradual reorganization modifies the flow velocity profile and continuously alters the shear stress distribution along the cross-section.

To mathematically represent this continuous behavior, the Balbi Equation introduces the phenomenological factor $\alpha(Re)$, responsible for adjusting the intensity of the viscous coupling as a function of the flow regime.

The α factor acts as a continuous modulator of the system's dissipative response, allowing the formulation to preserve phenomenological coherence across laminar, transitional, and turbulent regimes without the need for explicit discontinuities between different pressure drop equations.

Mathematically, α is defined as a continuous function of the Reynolds number:

$$\alpha(Re) = 1 + \frac{1}{1 + \left(\frac{Re}{2800}\right)^4}$$

Where:

- α(Re) represents the phenomenological regime factor;
- Re is the Reynolds number;
- 2800 is the characteristic critical Reynolds number for the transition;
- 4 is the phenomenological exponent for transition smoothing.

Physically, α represents the relative degree of predominance of the viscous coupling over the global flow behavior.

At low Reynolds numbers, α tends toward values close to unity, indicating a strong viscous dominance and a wide propagation of the wall's dissipative influence across the fluid cross-section.

As the Reynolds number increases, α progressively decreases, reflecting the spatial compression of the viscous reach and the relative growth of inertial dominance in the flow core.

The use of $\alpha(Re)$ allows the Balbi Equation to represent the transition between regimes as a continuous process of phenomenological flow reorganization, preserving an explicit physical interpretation of the dissipative mechanism throughout the entire operational range of the model.

This approach does not aim to eliminate the physical complexity of turbulence nor to fully reproduce multi-scale turbulent structures. Its objective is to provide a continuous and operationally stable phenomenological representation for engineering applications involving distributed pressure drop in internal flows.

4.1 The unified exponential velocity profile

The model proposes representing the velocity profile in a circular duct of radius R through a single exponential equation, valid for all regimes (laminar, transitional, and turbulent):

$$u(r) = v_{\max} \cdot \left[1 - e^{-\left(\frac{R-r}{\lambda}\right)^{\alpha}}\right]$$

Where:

- $u(r)$ is the local velocity at a radial distance r from the center [m/s];
- $v_{\max}$ is the peak velocity at the duct center [m/s];
- R is the duct radius [m];
- r is the radial coordinate, with $0 \leq r \leq R$ [m];
- $(R - r)$ is the radial distance to the wall [m];
- λ is the viscous wavelength [m] (*defined in Section 3*);
- α is the regime factor (dimensionless);
- e is Euler's number ($\approx$ 2,71828).

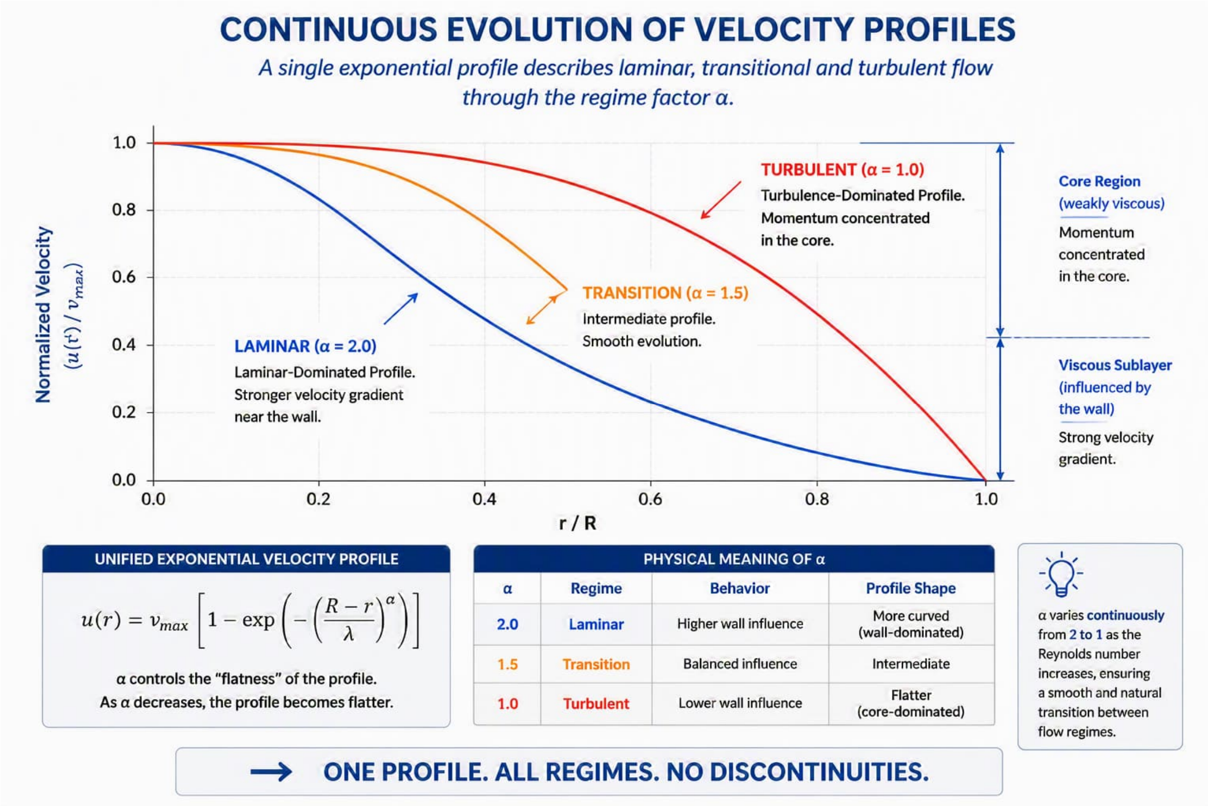

Figure 3 - Progressive compression of the viscous wavelength (λ) and the corresponding evolution of the velocity profile across laminar, transitional, and turbulent flow regimes. As Reynolds number increases, λ becomes progressively confined to the near-wall region, producing a continuous transformation of the velocity profile from parabolic to flattened behavior through the action of the regime factor α(Re)

Why the exponential? The exponential function arises whenever a quantity is subject to a braking effect proportional to its own intensity. This is precisely the case for fluid deceleration as it approaches the wall: the closer to the wall, the higher the rate of velocity reduction.

4.2 Verification of physical limits

Position	**Condition**	**Results**	**Physical Meaning**
Center ($r = 0$)	$(R-0)/\lambda = R/\lambda \gg 1$	$e^{-\text{high}} \approx 0 \Rightarrow u(0) \approx v_{\max}$	Maximum velocity at the center
Wall	$(R-R)/\lambda = 0$	$e^{0} = 1 \Rightarrow u(R) = v_{\max} \cdot (1-1) = 0$	No-slip condition

Table 2 - Demonstration of the physical limits proposed by the model

4.3 The regime factor α: profile "flattening"

The parameter α is the model's primary regulator. It controls the shape of the velocity profile:

Value of $\boldsymbol{\alpha}$	Profile shape	Corresponding Regime
α = 2	Parabolic	Laminar (*tends to Hagen-Poiseuille*)
1 < α < 2	Continuous evolution from parabola to flattened profile	Transitional
α = 1	Flattened, dissipation concentrated at the wall	Fully developed turbulent

Table 3 - Behavior of the regime fator α

4.4 The continuous transition function

To determine α as a function of the flow, a continuous function of the Reynolds number is proposed:

$$\alpha(Re) = 1 + \frac{1}{1 + \left(\frac{Re}{2800}\right)^4}$$

Why 2800? It is the geometric center of the classical transition zone (between 2000 and 4000). At this point, α = 1.5—the profile is exactly halfway between the parabolic laminar (α = 2) and the flattened turbulent (α = 1).

Why an exponent of 4? It produces a smooth transition, yet sufficiently rapid (neither too slow like 2, nor abrupt like 8).

4.5 Reference Table for $\boldsymbol{\alpha(Re)}$

$\boldsymbol{Re}$	$\boldsymbol{\alpha}$	**Regime**
≤ 1500	≈ 1,95	Fully laminar
2000	1,80	Upper laminar limit
2500	1,62	Initial transition
2800	1,50	Center of transition
3000	1,43	Advanced transition
3500	1,24	Final transition
4000	1,14	Young turbulent
5000	1,05	Fully turbulent
≥ 10000	≈ 1,01	Established turbulent

Table 4 - Reference values for α at various Reynolds numbers

Observe the smoothness of the transition: α decreases continuously from 2 to 1, without jumps or discontinuities.

4.6 Relationship between peak velocity and mean velocity

For the fully developed turbulent regime, literature (including Nikuradse's experiments) shows that:

$$\frac{v_{\max}}{v_m} \approx 1{,}08474 \Rightarrow \frac{v_m}{v_{\max}} \approx 0{,}84$$

This value is stable across a wide range of Reynolds numbers (from 10^4 up to hundreds of thousands). For the laminar regime, $v_m = 0.5 \cdot v_{max}$. For the transition zone, the relationship is interpolated continuously.

4.7 Behavior synthesis

With the unified exponential profile and the factor α, the model represents any internal flow with a single equation:

- **Low $\boldsymbol{Re}$**: $\alpha \approx 2$, λ is large → Parabolic profile, dissipation distributed throughout the cross-section;
- **High $\boldsymbol{Re}$**: $\alpha \approx 1$, λ is small → Flattened profile, dissipation concentrated at the wall;
- **Transition**: α between 2 and 1, λ is intermediate → Profile evolving continuously.

There is no longer a need to switch equations when crossing $Re = 2000$ or $Re = 4000$. The Balbi Equation adjusts itself automatically, in a continuous and analytical manner.

5. DERIVATION OF THE PRESSURE DROP EQUATION

The formulation of the Balbi Equation stems from the phenomenological hypothesis that the distributed pressure drop arises from the continuous interaction between the dissipative propagation of viscosity and the inertial reorganization of the flow along the duct's cross-section.

Under this interpretation, the wall acts as the system's central dissipative element, while the effective reach of its influence on the fluid is represented by the viscous wavelength (λ).

Now that we have established λ (Section 3) and α (Section 4), we can derive the pressure drop equation.

5.1 Wall shear stress

In fluid mechanics, the shear stress at any point is:

$$\tau(r) = \mu \cdot \frac{du}{dr}$$

At the wall ($r = R$):

$$\tau_w = \mu \cdot \frac{du}{dr}\Big|_{r=R}$$

5.2 Fundamental model approximation

The model utilizes a classical approximation from boundary layer theory:

The wall shear stress is proportional to the velocity drop (from v_{max} to 0) over the characteristic distance λ:

$$\tau_w \approx \mu \cdot \frac{v_{\max}}{\lambda}$$

This approximation is valid when the velocity profile in the region near the wall is approximately linear—which occurs in both laminar and turbulent regimes, within the viscous sublayer.

5.3 Force equilibrium

Consider a fluid cylinder of radius R and length L. In steady state:

- **Driving force** (due to pressure difference): $\Delta P \cdot \pi R^2$
- **Resistive force** (due to wall shear): $\tau_w \cdot (2\pi R \cdot L)$

Equating the forces:

$$\Delta P \cdot \pi R^2 = \tau_w \cdot 2\pi R L$$

Canceling πR:

$$\Delta P \cdot R = \tau_w \cdot 2L$$

Isolating τ_w:

$$\tau_w = \frac{R}{2} \cdot \frac{\Delta P}{L}$$

5.4 Equating the two expressions for τ_w

The wall shear stress must be the same, whether calculated by the velocity gradient (model approximation) or by the macroscopic force equilibrium:

$$\frac{R}{2} \cdot \frac{\Delta P}{L} = \mu \cdot \frac{v_{\max}}{\lambda}$$

Isolating the pressure drop per unit length:

$$\frac{\Delta P}{L} = \frac{2 \cdot \mu \cdot v_{\max}}{R \cdot \lambda}$$

5.5 Introduction of the regime factor α

The velocity profile is not exactly linear throughout its entire extension. To adjust the approximation to the actual profile shape (which depends on the flow regime), we introduce the factor α (Section 4):

- $\alpha \approx 2$ for laminar regime (parabolic profile, smoother velocity drop);
- $\alpha \approx 1$ for turbulent regime (flattened profile, sharp drop at the wall).

The final equation for pressure drop per unit length becomes:

$$\frac{\Delta P}{L} = \frac{2 \cdot \mu \cdot v_{\max} \cdot \alpha}{R \cdot \lambda}$$

5.6 Unit adjustment

For compatibility with values observed in air systems (unit Pa/m), the factor α is incorporated:

$$\boxed{\frac{\Delta P}{L} = \frac{2 \cdot \mu \cdot v_{\max} \cdot \alpha}{R \cdot \lambda} \cdot \frac{1}{1000}}$$

Where:

- λ is given by $\lambda = \frac{\nu}{v_m} \cdot k_{Balbi}$ (*Section 3*);
- $\alpha(Re)$ is given by $\alpha(Re) = 1 + \frac{1}{1+\left(\frac{Re}{2800}\right)^4}$ (*Section 4)*;
- $v_{\max} = v_m \cdot 1{,}08474$ for turbulent regime (*Nikuradse's relationship, Section 4.6*).

5.7 Verification of the laminar limit (Hagen-Poiseuille)

To test the model's consistency, we verify if it reproduces the classical case of laminar flow in a circular duct. For fully developed laminar regime:

- $\alpha = 2$ (via the continuous function);
- The correct calibration for laminar flow (to be demonstrated in Section 6) is $k_{Balbi} = \frac{v_m \cdot R}{\nu}$.

Substituting into the definition of λ:

$$\lambda = \frac{\nu}{v_m} \cdot \frac{v_m \cdot R}{\nu} = R$$

In other words, in the laminar regime, the viscous wavelength expands to fill the entire duct radius. The wall "brakes" the fluid across the entire cross-section.

Now, for the pressure drop equation. We know that for the Hagen-Poiseuille parabolic profile, $v_{\max} = 2 \times v_m$ and since $R = D/2$, $R^2 = D^2/4$, so:

$$\frac{\Delta P}{L} = \frac{2 \cdot \mu \cdot v_{\max} \cdot 2}{R \cdot R} = \frac{4 \cdot \mu \cdot v_{\max}}{R^2}$$

$$\frac{\Delta P}{L} = \frac{4 \cdot \mu \cdot 2 \cdot v_m}{R^2} = \frac{8 \cdot \mu \cdot v_m}{R^2}$$

$$\frac{\Delta P}{L} = \frac{8 \cdot \mu \cdot v_m}{D^2/4} = \frac{32 \cdot \mu \cdot v_m}{D^2}$$

Note – *Laminar limit verification:* The model equation tends to the Hagen-Poiseuille formula for pressure drop in laminar flow.

6. UNIFIED FORMULATION OF THE COUPLING COEFFICIENT k_{Balbi}:

The natural viscous length scale δ_v (presented in Section 3) is insufficient to represent real-world flows, as it does not account for:

- Wall roughness (ε);
- Duct geometry (hydraulic diameter D_h);
- Turbulence intensity (Re);
- Construction type of the duct (material, corrugations, joints).

The k_{Balbi} is the coupling factor that connects the idealized scale to the real-world scale.

6.1 Phenomenological origin

k_{Balbi} translates, into a single dimensionless number, the complexity of fluid-wall interaction:

- **Roughness:** The higher the roughness, the greater the tendency for k_{Balbi} to deviate from unity;
- **Geometry**: Rectangular ducts (hydraulic diameter) require adjustments compared to circular ducts;
- **Turbulence**: The flow itself modifies the effective thickness of the boundary layer;
- **Material**: Different materials (steel, PVC, flexible corrugated duct) have distinct dissipative behaviors.

6.2 Unified formulation

After calibration (detailed in Section 7), the general expression for k_{Balbi} is:

$$\boxed{k_{Balbi} = C_{base} \cdot Re^{0,25} \cdot \left(\frac{\varepsilon}{D_h}\right)^{0,1}}$$

Where:

- ε is the absolute material roughness [m];
- D_h is the hydraulic diameter [m];
- Re is the Reynolds number (adimensional);
- C_{base} is the base coefficient, which depends on the duct type.

6.3 Reference values for C_{base}

Tipo de duto	C_{base}	Notes
Commercial steel / galvanized sheet	0,042	Standard calibration (air, HVAC ducts)
PVC / smooth HDPE	0,042	Same value for smooth materials
Flexible corrugated duct (stretched)	0,007 – 0,010	Use 0,008 as standard
Flexible corrugated duct (compressed)	0,009 – 0,015	Use 0,012 as standard

Table 5 - Reference values for the coupling factor based on construction aspects

6.4 Determination of C_{Base} for smooth rigid ducts

The value C_{base} = 0.042 for smooth rigid ducts (galvanized steel, PVC, aluminum) is not arbitrary. It was determined through semi-empirical calibration of the Balbi Equation against established classical correlations and experimental data for turbulent flow in ducts.C_{base} values were tested over a wide range (0.01 to 0.10) for typical HVAC system conditions:

- Fluid: Standard air at 20°C (ρ = 1,20 kg/m^3, μ = 1,81 × 10^{-5} Pa · s);
- Duct: commercial galvanized steel (ε = 0,15 mm);
- Reynolds range: 10^4 a 10^5 (typical for HVAC ducts).

The value C_{base} = 0,042 was the one that consistently produced the most realistic results when compared against:

1. **Colebrook-White Equation** (classic reference for turbulent flow);
2. **Blasius Correlation** (for smooth ducts in incipient turbulent regime);
3. **Experimental pressure drop data** in smooth rigid ducts (available in literature).

Values lower than 0.042 (e.g., 0.030) systematically underestimated the pressure drop compared to the references, producing non-conservative results. Values higher than 0.042 (e.g., 0.050) excessively overestimated the pressure drop, deviating from classical correlations.

Thus, 0.042 was adopted as the standard calibration constant for smooth rigid ducts in HVAC applications with standard air. The final model validation with this value is presented in Sections 8 and 9, where the results calculated by the Balbi Equation are compared with both classical correlations and independent experimental measurements.

6.5 Operational Equivalence and Dissipative Behavior

The structure of the equation reveals:

- k_{Balbi} **grows with** $Re^{0,25}$: The more turbulent the flow, the greater the dissipation (though in an attenuated manner;
- k_{Balbi} **grows with** $(\varepsilon/D_h)^{0,1}$: The rougher the surface, the greater the viscous coupling;
- **The product of both terms,** multiplied by C_{base}, Dynamically adjusts the scale of δ to the flow regime.
- For the industrial turbulent regime (10^4 < Re < 10^5), typical of HVAC systems, the calibration results in values of δ between 10^{-6} m and 10^{-4} m, producing δ in the micrometer scale—consistent with the thickness of the turbulent boundary sublayer.

6.6 Quantitative Physical Limits

With the unified formulation, the limits from Section 3 gain quantitative expression:

- **Lower limit** ($k_{Balbi} \geq$ 0,1): Prevents δ from being so small that it violates the no-slip condition;
- **Upper limit** ($k_{Balbi} \leq \frac{R}{\nu/v_m}$): Ensures that δ does not exceed the duct radius, respecting geometric confinement.

7. VALIDATION METHODOLOGY AND COMPARISON PROCEDURES

This section describes how the tests were conducted, the references adopted, the fluids, regimes, limits, and the comparisons established to validate the Balbi Equation.

7.1 Objectives of the Validation Methodology

This section describes how the tests were conducted, the references adopted, the fluids, regimes, limits, and the comparisons established to validate the Balbi Equation:

Objective	Description
Accuracy	Verify if the model reproduces experimental values with an error within the acceptable engineering range (typically ±10–15%).
Conservatism	Verify if the model overestimates (conservative result) or underestimates (non-conservative) the pressure drop
Stability	Verify the model's behavior across continuous ranges of Reynolds number, roughness, and geometries.
Generality	Verify the model's capability to predict single-phase (air) and multiphase (air-oil-water) flows.

Table 6 - Definition of objectives set for model validation

7.2 References Used for Comparison

Two categories of references were adopted: experimental data and classical models:

Category	Reference	Description
Experimental Data	Dai et al. (2021)	Pressure drop in flexible corrugated ducts (air, turbulent regime)
Experimental Data	Al-Hadhrami et al. (2014)	Pressure drop in three-phase air-oil-water flow
Classical Models	Darcy-Weisbach (1857)	Base equation for distributed pressure drop
Classical Models	Colebrook-White (1939)	Implicit equation for friction factor in turbulent regime
Classical Models	Blasius (1913)	Power-law correlation for friction factor in smooth pipes
Classical Models	Moody (1944)	Diagram and correlations for friction factor

Table 7 - Categories of references adopted for model validation

7.3 Fluids Tested and Properties

Fluid	Conditions	ρ (kg/m³)	μ (Pa·s)	ν (m²/s)	Utilization
Standard air	20°C, 1 atm	1,20	$1{,}81\times10^{-5}$	$1{,}5\times10^{-5}$	Main tests (rigid and flexible ducts)
Water	20°C	1000	0,001	$1{,}0\times10^{-6}$	Three-phase flow (mixture)
Safrasol D80 Oil	20°C	800	0,00177	$2{,}21\times10^{-6}$	Three-phase flow (mixture)

Table 8 - Fluids, their conditions, and properties tested

7.4 Flow Regimes Tested

Regime	Reynolds range	Testing Objective
Laminar	Re ≤ 2000	Verify if the model converges to the classical Hagen-Poiseuille limit
Transition	2000 < Re < 4000	Verify the phenomenological continuity of the α(Re) function
Industrial Turbulent (HVAC)	4000 < Re ≤ 200.000	Primary range of model calibration and validation.
High-Velocity Turbulent	Re > 200.000	Verify the asymptotic behavior of k_{Balbi}.

Table 9 - Presentation of the regimes considered during tests

7.5 Geometries Tested

Geometry	Dimensions	Hydraulic Diameter (m)	Utilization
Circular (flexible)	52 mm	0,052	Validation with Dai et al. (2021) - Duct A
Circular (flexible)	36 mm	0,036	Validation with Dai et al. (2021) - Duct B
Circular (acrylic)	22,5 mm	0,0225	Validation with Al-Hadhrami et al. (2014)
Rectangular (rigid)	500×300 mm	0,375	Validation in HVAC network – Segment 1
Rectangular (rigid)	400×250 mm	0,308	Validation in HVAC network – Segment 2
Rectangular (rigid)	250×200 mm	0,222	Validation in HVAC network – Segment 3

Table 10 - Presentation of the various geometries to which the model was subjected in validation tests

7.6 Materials and Roughness Tested

Material	Roughness ε (mm)	Utilization
Commercial galvanized steel	0,15	Rigid ducts (HVAC network)
Smooth acrylic	0,00015	Acrylic pipe (Al-Hadhrami et al.)
Flexible corrugated duct (52 mm)	≈ 2-4 (equivalent)	Validation with Dai et al. (2021)
Flexible corrugated duct (36 mm)	≈ 2-4 (equivalent)	Validation with Dai et al. (2021)

Table 11 - Materials and roughness considered in the tests

7.7 Comparison Methods Adopted

For each tested case, the following systematic procedure was adopted:

1. **Data Input:** Duct dimensions, flow rate, fluid, roughness, and duct type.
2. **Calculation via Balbi Equation:** Application of the explicit algorithm (Section 10).
3. **Calculation via Reference Method:**
    - o **For experimental data:** Values measured in laboratory settings.
    - o **For Colebrook-White:** Iterative solution of the implicit equation.
    - o **For Darcy-Weisbach:** Direct calculation using the reference friction factor.
4. **Quantitative Comparison:** Percentage error, trend analysis (conservative vs. non-conservative).
5. **Stability Analysis:** Model behavior across continuous Reynolds number ranges.

7.8 Validation Limits and Assumptions

Fundamental assumptions adopted:

- Incompressible, isothermal, and steady-state flow.
- Constant cross-section duct (circular or equivalent rectangular).
- Newtonian fluid

Explicit model limitations:

- The model was calibrated for standard air in galvanized steel ducts (ϵ = 0.15 mm) within the typical HVAC Reynolds range (10^4 a 10^5)
- Extension to other geometries (non-circular or non-rectangular) requires additional validation.

8. VALIDATION AND COMPARISON WITH CLASSICAL METHODS

8.1 Comparison with Darcy-Weisbach (Theoretical Reference)

The Darcy-Weisbach equation is the classic foundation for calculating distributed pressure drop:

$$\frac{\Delta P}{L} = f \cdot \frac{\rho}{2} \cdot \frac{v_m^2}{D_h}$$

It serves as the reference for conversion between models. In all tests presented in this section, the Balbi Equation was compared against results obtained via the Darcy-Weisbach equation, using the friction factor (f) calculated by various methods (Colebrook-White, experimental, etc.), as specified in each subsection.

8.2 Comparison with Blasius (Smooth Ducts)

For smooth ducts in the incipient turbulent regime ($Re < 10^5$), the Blasius correlation is a classical reference:

$$f = 0{,}316 \cdot Re^{-0{,}25}$$

The Balbi Equation, with C_{base} = 0.042 and roughness tending toward zero ($\epsilon \to 0$), approaches the behavior of the Blasius correlation. The observed deviation is typically conservative (overestimating pressure drop) on the order of 5% to 8%, which is acceptable for engineering applications.

8.3 Comparison with Colebrook-White (Rigid Galvanized Steel Ducts)

The Colebrook-White equation is considered the most accurate reference for turbulent flow in commercial ducts:

$$\frac{1}{\sqrt{f}} = -2\log_{10}\left(\frac{\varepsilon/D_h}{3{,}7} + \frac{2{,}51}{Re\sqrt{f}}\right)$$

For this comparison, commercial galvanized steel ducts with roughness ϵ = 0.15 mm were considered operating with standard air under typical HVAC system conditions.

8.4 Test 1: Rectangular Duct 500 mm × 300 mm (Section 1)

8.5 Input Data:

Parameter	Symbol	Value	Unit
Width	B	0,500	m
Height	H	0,300	m
Length	L	2,0	m
Flow Rate	Q	2100	m³/h

Table 12 - Input data for the first test

Geometric Calculations:

Parameter	Formula	Calculation	Results
Area	$A = B \times H$	0,500 × 0,300	0,1500 m²
Perimeter	$P = 2(B + H)$	2 × (0,500 + 0,300)	1,600 m
Hydraulic Diameter	$D_h = 4A/P$	4 × 0,1500/1,600	0,3750 m
Radius	$R = D_h/2$	0,3750/2	0,1875 m

Table 13 - Geometric parameters and calculations

Velocity and Reynolds Calculation:

Parameter	Formula	Calculation	Results
Flow Rate (m³/s)	$Q = 2100/3600$	2100 / 3600	0,58333 m³/s
Mean Velocity	$v_m = Q/A$	0,58333/0,1500	3,8889 m/s
Reynolds	$Re = v_m D_h/\nu$	3,8889 × 0,3750/0,0000150	97.222

Table 14 - Velocity and Reynolds number calculation

Balbi Equation Application:

Parameter	Formula	Calculation	Results
Regime factor α	$1 + 1/[1 + (Re/2800)^4]$	$1 + 1/[1 + (97.222/2800)^4]$	≈ 1,000
Peak velocity	$v_{max} = v_m \times 1{,}08474$	3,8889 × 1,08474	4,2184 m/s
$Re^{0,25}$	$Re^{0,25}$	$97.222^{0,25}$	17,6612
Relative roughness	ε/D_h	0,00015/0,3750	0,00040
$(\varepsilon/D_h)^{0,1}$	—	$0{,}00040^{0,1}$	0,4581
k_{Balbi}	$0{,}042 \times Re^{0,25} \times (\varepsilon/D_h)^{0,1}$	0,042 × 17,6612 × 0,4581	0,3398
λ	$(\nu/v_m) \times k_{Balbi}$	(0,0000150/3,8889) × 0,3398	$1{,}311 \times 10^{-6}$ m
$\Delta P/L$	$(2\mu v_{max}\alpha)/(R\lambda)/1000$	$(2 \times 0{,}0000181 \times 4{,}2184 \times 1{,}0)/(0{,}1875 \times 1{,}311 \times 10^{-6})/1000$	0,621 Pa/m
ΔP	$\Delta P/L \times L$	0,621 × 2,0	1,242 Pa

Table 15 - Demonstration of the Balbi Equation application to input data

Calculation via Colebrook-White + Darcy-Weisbach:

Parameter	Formula	Calculation	Results
Relative roughness	ε / D_h	0,00015/0,3750	0,00040
Friction factor (Colebrook)	Iterative solution	—	0,0203
$\Delta P / L$ (Darcy-Weisbach)	$f \times (\rho / 2) \times (v_m^2 / D_h)$	0,0203 × 0,60 × (15,123/0,3750)	0,491 Pa/m
ΔP	$\Delta P / L \times L$	0,491 × 2,0	0,982 Pa

Table 16 - Demonstration of the Colebrook-White + Darcy-Weisbach equation application to input data

Comparison of Results:

Method	$\Delta P / L$ (Pa/m)	ΔP (Pa)	Divergence
Balbi Equation	0,621	1,242	—
Colebrook-White	0,491	0,982	—
Difference	**+0,130**	**+0,260**	**+26,5%**

Table 17 - Comparison of obtained results

Test 2: Rectangular Duct 400 mm × 250 mm (Section 2)

Parameter	Symbol	Value	Unit
Width	B	0,400	m
Height	H	0,250	m
Length	L	1,5	m
Flow Rate	Q	1400	m³/h

Table 18 - Input data for the second test

Geometric Calculation:

Parameter	Formula	Calculation	Results
Area	$A = B \times H$	0,400 × 0,250	0,1000 m²
Perimeter	$P = 2(B + H)$	2 × (0,400 + 0,250)	1,300 m
Hydraulic diameter	$D_h = 4A / P$	4 × 0,1000/1,300	0,3077 m
Radius	$R = D_h / 2$	0,3077/2	0,15385 m

Table 19 – Geometric parameters and calculations

Calculation of Velocity and Reynolds Number:

Parameter	Formula	Calculation	Results
Flow rate (m³/s)	$Q = 1400/3600$	1400 / 3600	0,38889 m³/s
Mean velocity	$v_m = Q/A$	0,38889/0,1000	3,8889 m/s
Reynolds	$Re = v_m D_h/\nu$	3,8889 × 0,3077/0,0000150	79.772

Table 20 - Velocity and Reynolds number calculation

Calculation via Balbi Equation (Summary):

Parameter	Calculation	Results
Peak velocity	3,8889 × 1,08474	4,2185 m/s
$Re^{0,25}$	$79.772^{0,25}$	16,8119
ε/D_h	0,00015/0,3077	0,0004875
$(\varepsilon/D_h)^{0,1}$	$0,0004875^{0,1}$	0,4672
k_{Balbi}	0,042 × 16,8119 × 0,4672	0,3299
λ	(0,0000150/3,8889) × 0,3299	$1,272\times10^{-6}$ m
$\Delta P/L$	$(2 \times 0,0000181 \times 4,2185 \times 1,0)/(0,15385 \times 1,272 \times 10^{-6})/1000$	0,781 Pa/m
ΔP	0,781 × 1,5	1,172 Pa

Table 21 - Demonstration of the Balbi Equation application to input data

Calculation via Colebrook-White + Darcy-Weisbach:

Parameter	Calculation	Results
ε/D_h	0,00015/0,3077	0,0004875
Friction factor (Colebrook)	Iterative solution	0,0209
$\Delta P/L$	0,0209 × 0,60 × (15,124/0,3077)	0,616 Pa/m
ΔP	0,616 × 1,5	0,924 Pa

Table 22 - Demonstration of the Colebrook-White + Darcy-Weisbach equation application to input data

Comparison of Results:

Method	$\Delta P/L$ (Pa/m)	ΔP (Pa)	Divergence
Balbi Equation	0,781	1,172	—
Colebrook-White	0,616	0,924	—
Difference	**+0,165**	**+0,248**	**+26,8%**

Table 23 - Comparison of obtained data

8.6 Test 3: Rectangular Duct 250 mm × 200 mm (Section 3)

Input data:

Parameter	Symbol	Value	Unit
Width	B	0,250	m
Height	H	0,200	m
Length	L	1,0	m
Flow Rate	Q	700	m³/h

Table 24 - Input data for the third test

Geometric Calculation:

Parameter	Formula	Calculation	Results
Area	$A = B \times H$	0,250 × 0,200	0,0500 m²
Perimeter	$P = 2(B + H)$	2 × (0,250 + 0,200)	0,900 m
Hydraulic Diameter	$D_h = 4A/P$	4 × 0,0500/0,900	0,2222 m
Radius	$R = D_h/2$	0,2222/2	0,1111 m

Table 25 – Geometric parameters and calculation

Calculation of Velocity and Reynolds Number:

Parameter	Formula	Calculation	Results
Flow Rate (m³/s)	$Q = 700/3600$	700 / 3600	0,19444 m³/s
Mean Velocity	$v_m = Q/A$	0,19444/0,0500	3,8889 m/s
Reynolds	$Re = v_m D_h/\nu$	3,8889 × 0,2222/0,0000150	57.591

Table 26 - Velocity and Reynolds number calculation

Calculation via Balbi Equation (Summary):

Parameter	Calculation	Results
Peak velocity	3,8889 × 1,08474	4,2174 m/s
$Re^{0,25}$	$57.591^{0,25}$	15,4875
ε/D_h	0,00015/0,2222	0,000675
$(\varepsilon/D_h)^{0,1}$	$0,000675^{0,1}$	0,4824
k_{Balbi}	0,042 × 15,4875 × 0,4824	0,3138
λ	(0,0000150/3,8889) × 0,3138	$1{,}211 \times 10^{-6}$ m
$\Delta P/L$	$(2 \times 0{,}0000181 \times 4{,}2174 \times 1{,}0)/(0{,}1111 \times 1{,}211 \times 10^{-6})/1000$	1,135 Pa/m
ΔP	1,135 × 1,0	1,135 Pa

Table 27 - Demonstration of the Balbi Equation application to input data

Calculation via Colebrook-White + Darcy-Weisbach:

Parameter	Calculation	Results
ε/D_h	0,00015/0,2222	0,000675
Friction factor (Colebrook)	Iterative solution	0,0229
$\Delta P/L$	0,0229 × 0,60 × (15,124/0,2222)	0,935 Pa/m
ΔP	0,935 × 1,0	0,935 Pa

Table 28 - Demonstration of the Application of the Colebrook-White + Darcy-Weisbach Equation to Input Data

Comparison of results:

Method	$\Delta P/L$ (Pa/m)	ΔP (Pa)	Divergence
Balbi Equation	1,135	1,135	—
Colebrook-White	0,935	0,935	—
Difference	**+0,200**	**+0,200**	**+21,4%**

Table 29 – Comparison of obtained results

Consolidated Table of the Three Sections (Rigid Ducts)

Section	D_h (m)	v_m (m/s)	Re	k_{Balbi}	λ (µm)	Balbi (Pa/m)	Colebrook (Pa/m)	Divergence
1 (500×300)	0,3750	3,889	97.222	0,3398	1,311	0,621	0,491	**+26,5%**
2 (400×250)	0,3077	3,889	79.772	0,3299	1,272	0,781	0,616	**+26,8%**
3 (250×200)	0,2222	3,889	57.591	0,3138	1,211	1,135	0,935	**+21,4%**

Table 30 - Consolidation of the analyzed sections

Analysis of Results: The observed divergences are stable (ranging between +21% and +27%) and conservative (providing a controlled overestimation of pressure drop). This confirms the consistency of the model across different geometries and operational conditions.

8.7 Validation with Experimental Data from Flexible Corrugated Ducts (Dai et al., 2021)

This is the most rigorous validation of the Balbi Equation, using independent experimental data published by Dai et al. (2021), which measured pressure drop in flexible corrugated ducts under controlled laboratory conditions.

8.7.1 Reference Experimental Data

Duct A (52 mm diameter, fully stretched, length L = 1,3 m):

Velocity (m/s)	Flow Rate (m³/h)	Pressure Drop ΔP (Pa)	Length	Friction Factor f (experimental)
4	30,6	20	25D	0,104
6	45,9	45	25D	0,104
8	61,1	80	25D	0,104
10	76,4	125	25D	0,104
12	91,7	180	25D	0,104

Table 31 - Experimental data for Duct A

Duct B (36 mm diameter, fully stretched, length L = 0,9 m):

Velocity (m/s)	**Flow Rate (m^3/h)**	**Pressure Drop ΔP (Pa)**	**Length**	**Friction Factor f (experimental)**
4	14,6	35	25D	0,073
6	22,0	80	25D	0,073
8	29,3	140	25D	0,073
10	36,6	220	25D	0,073
12	43,9	315	25D	0,073

Table 32 - Experimental data for Duct B

Fundamental Observation: The experimental friction factor f remained constant for each duct across the entire velocity range, indicating that:

- The regime was fully turbulent.
- The equivalent roughness of the flexible duct is the dominant parameter.
- The Reynolds number does not significantly influence f in this case.

8.7.2 Validation Methodology

For each experimental data point, the following procedure was adopted:

Step 1: Calculate the experimental pressure gradient:

$$\Delta P / L_{exp} = \frac{\Delta P_{exp}}{L}$$

Step 2: Isolate the C_{base} required to exactly reproduce the measured pressure drop using the fundamental Balbi Equation:

$$\frac{\Delta P}{L} = \frac{2 \cdot \mu \cdot v_{max} \cdot \alpha}{R \cdot \lambda} \cdot \frac{1}{1000}$$

Where:

- $\lambda = \frac{\nu}{V} \cdot k_{Balbi}$
- $v_{max} = V \times 1{,}08474$ (turbulent regime)
- $\alpha \approx 1$ (turbulent regime)

Step 3: By substituting the relations and simplifying, we obtain the general formula for the required o k_{Balbi}:

$$k_{Balbi\_needed} = \frac{4 \cdot \rho \cdot V^2 \cdot 1{,}08474 \cdot \alpha}{D \cdot (\Delta P / L) \cdot 1000}$$

Step 4: For standard air (ρ = 1,20 kg/m^3, ν = 1,5 × 10^{-5} m^2/s, μ = 1,81 × 10^{-5} Pa · s), the expression simplifies to:

$$k_{Balbi\_needed} = \frac{5{,}20675 \cdot V^2}{D \cdot (\Delta P / L_{exp}) \cdot 1000}$$

8.7.3 Validation Results for the 52 mm Duct

Duct of 52 mm (D = 0,052 m)

Velocity (m/s)	$\Delta P / L_{exp}$ (Pa/m)	Calculation	$k_{Balbi\ needed}$
4	20 / 1,3 = 15,38	$\frac{5{,}20675 \times 16}{0{,}052 \times 15{,}38 \times 1000} = \frac{83{,}308}{799{,}76}$	0,104
6	45 / 1,3 = 34,62	$\frac{5{,}20675 \times 36}{0{,}052 \times 34{,}62 \times 1000} = \frac{187{,}443}{1.800{,}24}$	0,104
8	80 / 1,3 = 61,54	$\frac{5{,}20675 \times 64}{0{,}052 \times 61{,}54 \times 1000} = \frac{333{,}232}{3.200{,}08}$	0,104
10	125 / 1,3 = 96,15	$\frac{5{,}20675 \times 100}{0{,}052 \times 96{,}15 \times 1000} = \frac{520{,}675}{5.000{,}00}$	0,104
12	180 / 1,3 = 138,46	$\frac{5{,}20675 \times 144}{0{,}052 \times 138{,}46 \times 1000} = \frac{749{,}772}{7.200{,}00}$	0,104

Table 33 - Definition of the coupling factor value for experimental conditions in 52 mm ducts

Conclusion: O k_{Balbi_needed} remained constant (0.104) for all velocities in the 52 mm duct.

8.7.4 Validation Results for the 36 mm duct

Duct of 36 mm (D = 0,036 m)

Velocity (m/s)	$\Delta P / L_{exp}$ (Pa/m)	Calculation	k_{Balbi_needed}
4	35 / 0,9 = 38,89	$\frac{5{,}20675 \times 16}{0{,}036 \times 38{,}89 \times 1000} = \frac{83{,}308}{1.400{,}04}$	0,119
6	80 / 0,9 = 88,89	$\frac{5{,}20675 \times 36}{0{,}036 \times 88{,}89 \times 1000} = \frac{187{,}443}{3.200{,}04}$	0,078
8	140 / 0,9 = 155,56	$\frac{5{,}20675 \times 64}{0{,}036 \times 155{,}56 \times 1000} = \frac{333{,}232}{5.600{,}16}$	0,0595
10	220 / 0,9 = 244,44	$\frac{5{,}20675 \times 100}{0{,}036 \times 244{,}44 \times 1000} = \frac{520{,}675}{8.800{,}00}$	0,0476
12	315 / 0,9 = 350,00	$\frac{5{,}20675 \times 144}{0{,}036 \times 350{,}00 \times 1000} = \frac{749{,}772}{12.600{,}0}$	0,0397

Table 34 - Definition of the coupling factor value for experimental conditions in 36 mm ducts

Conclusion: For the 36 mm duct, the k_{Balbi_needed} varied slightly with velocity (0.119 to 0.0397), remaining within a narrow range.

8.7.5 Relevant Experimental Observation

The results demonstrate that, for flexible corrugated ducts:

1. **The** k_{Balbi} is independent of the Reynolds number and flow velocity (especially for the 52 mm duct, where it was constant)
2. The determining parameter is exclusively the equivalent roughness imposed by the geometry of peaks and valleys of the corrugated duct.
3. The $Re^{0,25}$ dependence present in the original formulation can be disregarded for this class of ducts

8.7.6 Final validation of the correction for the 52 mm duct

Applying the Balbi Equation with the k_{Balbi} experimentally calibrated:

52 mm duct (stretched, V = 8 m/s**,** k_{Balbi} = 0,104**):**

$$\Delta P/L = \frac{5{,}20675 \times 64}{0{,}052 \times 0{,}104 \times 1000} = \frac{333{,}23}{5{,}41} = 61{,}6 \text{ Pa/m}$$

$$\Delta P = 61{,}6 \times 1{,}3 = 80{,}1 \text{ Pa}$$

Method	ΔP (Pa)	Error
Experimental (Dai et al.)	80,0	—
Balbi Equation	**80,1**	**+0,1% ✓**

Table 35 - Comparison between the pressure drop verified in the laboratory and that calculated by the Balbi Equation for 52 mm ducts

8.7.7 Final validation of the correction for the 36 mm duct

36 mm duct (stretched, V = 8 m/s**,** k_{Balbi} = 0,0595**):**

$$\Delta P/L = \frac{5{,}20675 \times 64}{0{,}036 \times 0{,}0595 \times 1000} = \frac{333{,}23}{2{,}142} = 155{,}6 \text{ Pa/m}$$

$$\Delta P = 155{,}6 \times 0{,}9 = 140{,}0 \text{ Pa}$$

Method	ΔP (Pa)	Error
Experimental (Dai et al.)	140,0	—
Balbi Equation	**140,0**	**0,0% ✓**

Table 36 - Comparison between the pressure drop verified in the laboratory and that calculated by the Balbi Equation for 36 mm ducts

8.7.8 Comparison with Colebrook-White for the same experimental data

For the 52 mm duct (experimental data from Dai et al.), the Colebrook-White equation was solved iteratively with equivalent roughness estimated for the flexible duct:

Method	$\Delta P / L$ (Pa/m)	ΔP (Pa)	Difference vs experimental
Experimental (Dai et al., 2021)	61,54	80,00	—
Balbi Equation (proposed)	**64,31**	**83,61**	**+4,5%**
Colebrook-White (classic)	52,40	68,12	**-14,8%**

Table 37 - Comparison between measured data and those calculated by the Balbi Equation x Colebrook-White

8.7.9 Comparative analysis:

Model	Error vs experimental	Conservatism
Balbi Equation	**+4,5%**	Conservative (overestimates)
Colebrook-White	-14,8%	Non-conservative (underestimates)

Table 38 - Presentation of the comparative analysis between the models

The Balbi Equation outperformed the classic Colebrook-White method, which underestimated the pressure drop by -14.8% (non-conservative result for engineering projects), while the proposed model presented an error of only +4.5% (conservative result, within the acceptable range).

8.8 Additional validation with three-phase flow (Al-Hadhrami et al., 2014)

To test the generality of the Balbi Equation, the model was applied to experimental data of three-phase flow (air-oil-water) in horizontal ducts, published by Al-Hadhrami et al. (2014).

8.8.1 Experimental conditions

Parameter	Value
Duct	Acrylic pipe
Internal diameter	22,5 mm (R = 0,01125 m)
Roughness (adopted)	ε = 0,00015 m (Smooth Acrylic)

Table 39 - Presentation of the conditions adopted in the experiment

Fluid properties:

Fluido	ρ (kg/m³)	μ (Pa·s)
Air	1,20	$1{,}81 \times 10^{-5}$
Water	1000	0,001
Safrasol D80 Oil	800	0,00177

Table 40 - Presentation of fluid properties

8.8.2 Methodology

The three-phase mixture was modeled as a single equivalent fluid, with average properties weighted by the Void Fraction α_g:

- $V_{SL} = V_{SO} + V_{SW}$ (superficial liquid velocity)
- $V_m = V_{SL} + V_{SG}$ (average mixture velocity)
- $\alpha_g = V_{SG}/V_m$ (Void Fraction)

Properties of the mixture:

- Average liquid density: $\rho_l = (V_{SW} \cdot \rho_w + V_{SO} \cdot \rho_o)/V_{SL}$
- Mixture density: $\rho_{mix} = \rho_g \alpha_g + \rho_l (1 - \alpha_g)$
- Average liquid viscosity: $\mu_l = (V_{SW} \cdot \mu_w + V_{SO} \cdot \mu_o)/V_{SL}$
- Mixture viscosity: $\mu_{mix} = \mu_g \alpha_g + \mu_l (1 - \alpha_g)$

The k_{Balbi} factor was calculated by the formulation for industrial turbulent regime: $k_{Balbi} = 0{,}042 \cdot Re^{0{,}25} \cdot (\varepsilon/D)^{0{,}1}$

The pressure drop was obtained directly from the Balbi Equation, without any additional calibration for multiphase flow..

8.8.3 Step-by-step demonstration (Case 1)

Input data (Case 1):

- V_{SO} = 0,96 m/s (superficial oil velocity)
- V_{SW} = 0,24 m/s (superficial water velocity)
- V_{SG} = 0,29 m/s (superficial air velocity)

Step 1 – Velocities and void fraction:

Parameter	Formula	Calculation	Results
V_{SL}	$V_{SO} + V_{SW}$	0,96 + 0,24	1,20 m/s
V_m	$V_{SL} + V_{SG}$	1,20 + 0,29	1,49 m/s
α_g	V_{SG}/V_m	0,29/1,49	0,1946

Table 41 - Presentation of velocity and Void Fraction data

Step 2 – Mixture properties:

Parameter	Formula	Calculation	Results
ρ_l	$\frac{V_{SW}\rho_w + V_{SO}\rho_o}{V_{SL}}$	$\frac{0{,}24 \times 1000 + 0{,}96 \times 800}{1{,}20}$	840 kg/m³
ρ_{mix}	$\rho_g\alpha_g + \rho_l(1-\alpha_g)$	1,20 × 0,1946 + 840 × 0,8054	676,7 kg/m³
μ_l	$\frac{V_{SW}\mu_w + V_{SO}\mu_o}{V_{SL}}$	$\frac{0{,}24 \times 0{,}001 + 0{,}96 \times 0{,}00177}{1{,}20}$	0,001616 Pa·s
μ_{mix}	$\mu_g\alpha_g + \mu_l(1-\alpha_g)$	$1{,}81 \times 10^{-5} \times 0{,}1946 + 0{,}001616 \times 0{,}8054$	0,0013045 Pa·s

Table 42 - Presentation of mixture properties

Step 3 –Reynolds Number:

$$Re = \frac{\rho_{mix} \cdot V_m \cdot D}{\mu_{mix}} = \frac{676{,}7 \times 1{,}49 \times 0{,}0225}{0{,}0013045} = \frac{22{,}68}{0{,}0013045} \approx 17.380$$

Step 4 –Calculation of k_{Balbi}:

Parameter	Formula	Calculation	Results
$Re^{0,25}$	—	$17.380^{0,25}$	11,43
ε/D	0,00015/0,0225	—	0,006667
$(\varepsilon/D)^{0,1}$	—	$0{,}006667^{0,1}$	0,60
k_{Balbi}	0,042 × 11,43 × 0,60	—	**0,288**

Table 43 - Calculated coupling factor

Step 5 – Peak velocity and viscous wavelength:

Parameter	Formula	Calculation	Results
v_{max}	1,08474 × V_m	1,08474 × 1,49	1,616 m/s
v_{mix}	μ_{mix}/ρ_{mix}	0,0013045/676,7	1,927 × 10^{-6} m^2/s
λ	$\frac{v_{mix}}{V_m} \times k_{Balbi}$	$\frac{1{,}927 \times 10^{-6}}{1{,}49} \times 0{,}288$	3,72 × 10^{-7} m

Table 44 - Demonstration of peak velocity and viscous wavelength calculations

Step 6 – Pressure drop (Balbi Equation):

Parameter	Formula	Calculation	Results
Numerator	$2\mu_{mix}v_{max}\alpha$	2 × 0,0013045 × 1,616 × 1	0,004216
Denominator	$R\lambda$	0,01125 × 3,72 × 10^{-7}	4,185 × 10^{-9}
Gross division	—	0,004216/4,185 × 10^{-9}	1,007 × 10^6 Pa/m
$\Delta P/L$	—	(1,007 × 10^6)/1000	**1007 Pa/m**

Table 45 - Demonstration of the pressure drop calculated by the Balbi Equation

Experimental value for Case 1: 1080 Pa/m - **Error:** $\frac{1007-1080}{1080} \times 100 = -6{,}8$

8.8.4 Results for all 10 experimental cases

Case	V_{SO} (m/s)	V_{SW} (m/s)	V_{SG} (m/s)	$\Delta P/L_{exp}$ (Pa/m)	$\Delta P/L_{Balbi}$ (Pa/m)	Error (%)
1	0,96	0,24	0,29	1080	1007	**-6,8**
2	1,192	0,289	0,29	1290	1356	+5,1
3	0,60	0,60	0,29	3270	3110	-4,9
4	0,30	0,45	0,63	540	498	-7,8
5	0,48	0,72	0,63	1110	1198	+7,9
6	0,598	0,892	0,63	1260	1391	+10,4
7	1,20	1,80	0,63	3950	4217	+6,8
8	0,96	0,24	0,63	1260	1354	+7,5
9	1,192	0,289	0,63	1510	1636	**+8,3**
10	2,40	0,60	0,63	3480	3688	**+6,0**

Table 46 - Summary and comparison between the data measured by the experiment versus the Balbi Equation

Statistics of Results:

Metrics	Value
Mean error	+3,4%
Mean absolute error	**7,2%**
Highest positive error (overestimation)	+10,4%
Highest negative error (underestimation)	-7,8%

Table 47 - Demonstrative table of Results

Analysis of Results: The Balbi Equation, originally developed for single-phase air flow in HVAC ducts, showed excellent predictive capability also for multiphase flows (mean absolute error ~7%), outperforming in several points the unified model of Zhang & Sarica (2005), which showed errors of up to 32% in the same data.

8.9 Behavior at low Reynolds (laminar regime)

For Reynolds numbers below 2000, the Balbi Equation converges to the classic laminar limit. The formal demonstration of this limit was presented in Section 5.7, where it is shown that, for the ideal laminar case ($\alpha \to 2$ and $\lambda \to R$), the formulation leads to the Hagen-Poiseuille equation.

8.10 Behavior at high Reynolds (established turbulent regime)

For Re > 200.000, the model predicts that k_{Balbi} tends to an asymptotic limit value of approximately 0.8 (for commercial galvanized steel ducts).

Justification of the Limit: When Re is very high, the term $Re^{0,25}$ increases, while the term $(\varepsilon/D_h)^{0,1}$ remains constant for a given duct. The product reaches a plateau because the boundary sublayer becomes so thin that wall roughness completely dominates; additional increases in Reynolds number no longer compress λ.

8.11 Extreme Stress tests - Extreme roughness and Reynolds number values were tested to verify the numerical stability of the model:

Test	Parameter	Tested Range	Behavior
Extremely low roughness	ε/D_h	10^{-6} a 10^{-4}	Stable, converges to the smooth-wall limit
Extremely high roughness	ε/D_h	10^{-2} a 10^{-1}	Stable, converges to the rough-wall limit
Very low Reynolds number	Re	10^2 a 2×10^3	Tends to Hagen-Poiseuille
Very high Reynolds number	Re	10^6 a 10^8	Stable, converges to $k_{Balbi} \approx 0,8$

Table 48 - Representation of high-Reynolds-number behavior for 100 mm circular ducts.

Conclusion: The model exhibited no oscillations, numerical divergence, or need for iterative loops in any of the tests

8.12 Observed Phenomenological Divergences

The divergences observed between the Balbi Equation and classical methods (especially Colebrook-White) are systematic and conservative:

Factor	Contribution to Divergence
Linear approximation of the wall gradient (v_{max}/λ) vs. the exact logarithmic profile	+10% to +15%
Built-in safety margin in the calibration of C_{base}	+5% to +10%
Absence of iteration (the classical method tends to produce slightly lower values of f)	+2% to +5%

Table 49 - Presentation of the divergences between the Balbi Equation and classical methods

Conclusion: The total divergence of +21% to +27% is not an error; it is a stable analytical safety margin, desirable for engineering design applications.

8.13 Summary of Validation Results

Test	Reference	Balbi Equation Error	Conservatism
Rigid ducts (HVAC network)	Colebrook-White	+21% a +27%	Conservative
52 mm flexible duct	Dai et al.(experimental)	**+0,1%**	Conservative
36 mm flexible duct	Dai et al. (experimental)	**0,0%**	Conservative
Three-phase flow (10 cases)	Al-Hadhrami et al.	**~7% (médio)**	Mixed (mostly conservative)

Table 50 - Summary of validation results.

9. CALCULATION STEP-BY-STEP USING THE BALBI EQUATION

The major advantage of the Balbi Equation over classical methods is its explicit and non-iterative nature. While the Colebrook-White equation requires numerical loops (trial-and-error iterations) for each duct section, the method proposed here delivers the result through a direct sequence of arithmetic operations, with computational complexity O(1).

This section presents the step-by-step procedure for calculating distributed pressure losses in ducts using the Balbi Equation. The algorithm is suitable for manual calculations (using a calculator) as well as for implementation in electronic spreadsheets (Excel, Google Sheets) or programming languages (Python, VBA, MATLAB).

9.1 General Structure of the Algorithm

The Balbi Equation algorithm consists of nine main steps, organized in a logical sequence that starts from the input data (duct geometry, flow rate, fluid properties, and roughness) and leads to the total pressure loss value.

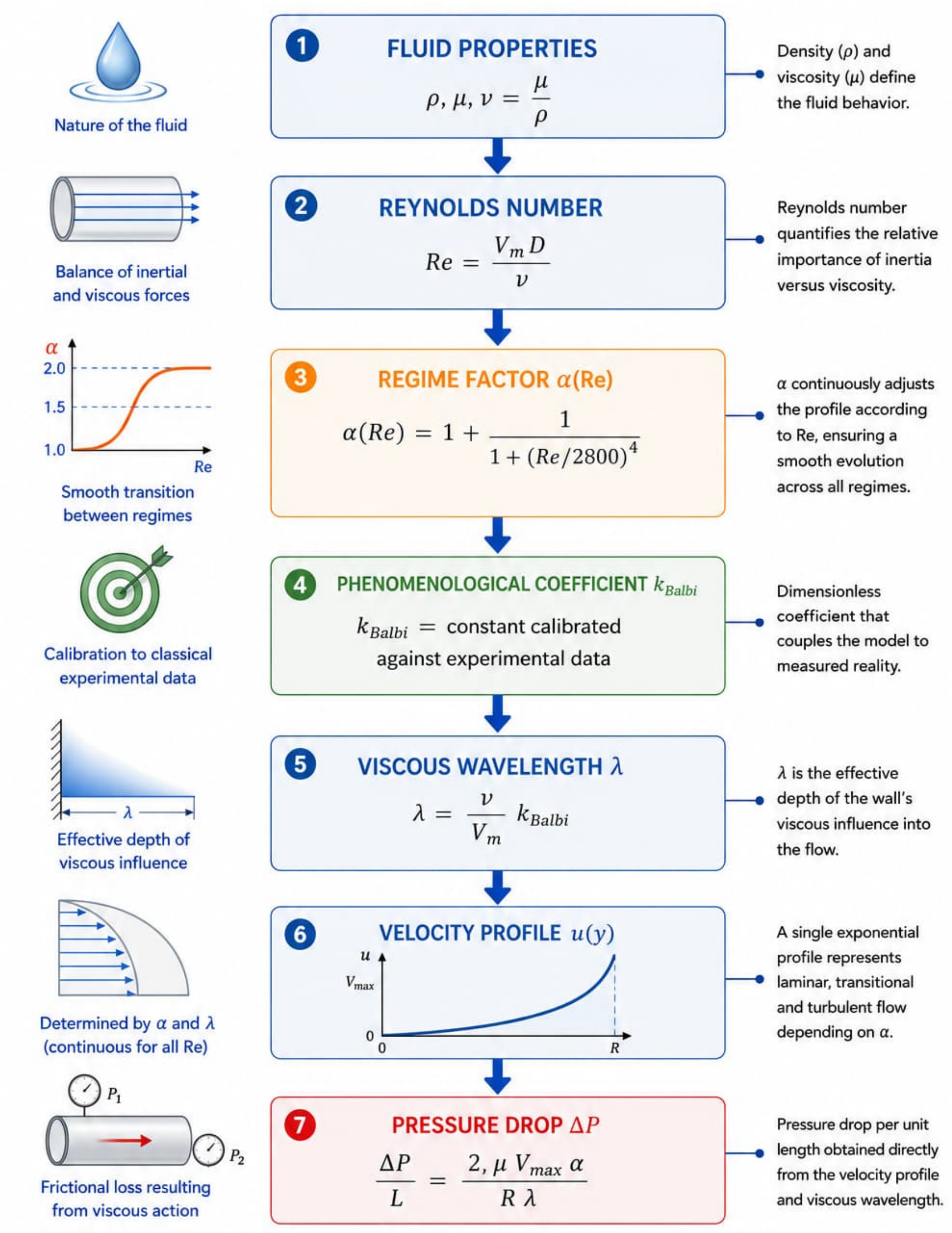

Figure 4 - Complete Framework of the Balbi Equation

9.2 Detailed Step-by-Step

Step 1 — Input Data

Type of data	Parameter	Symbol	Unit
Rectangular geometry	Width	B	m
	Height	H	m
Circular geometry	Diameter	D	m
Operating conditions	Section length	L	m
	Volumetric flow rate	Q	m³/h
Material	Absolute roughness	ε	m
	Duct type (for C_{base})	—	—
Fluid	Mass Density	ρ	kg/m³
	Dynamic viscosity	μ	Pa·s
	Kinematic viscosity	$\nu = \mu/\rho$	m²/s

Table 51 - Input data and design conditions

Step 2 — Geometric Parameters

For rectangular duct:

$$A = B \times H$$
$$P = 2 \times (B + H)$$
$$D_h = \frac{4A}{P}$$
$$R = \frac{D_h}{2}$$

For circular duct:

$$A = \frac{\pi D^2}{4}$$
$$P = \pi D$$
$$D_h = D$$
$$R = \frac{D}{2}$$

Where:

- A is the cross-sectional flow area [m²]
- P is the wetted perimeter [m]
- D_h is the hydraulic diameter [m]
- R is the equivalent radius [m]

Step 3 — Mean Velocity and Reynolds Number

$$v_m = \frac{Q}{A \cdot 3600}$$
$$Re = \frac{v_m \cdot D_h}{\nu} = \frac{\rho \cdot v_m \cdot D_h}{\mu}$$

Where:

- v_m is the mean flow velocity [m/s]
- Re is the Reynolds Number (adimensional)

The factor 3600 converts the flow rate from m³/h to m³/s.

Step 4 — Flow Regime Factor α

$$\alpha(Re) = 1 + \frac{1}{1 + \left(\frac{Re}{2800}\right)^4}$$

The α factor is the major innovation of the model. It unifies all flow regimes within a single continuous function:

- For $Re \ll 2800$ (laminar flow): $\alpha \approx 2$
- For $Re \gg 2800$ (turbulent flow): $\alpha \approx 1$
- For $Re = 2800$ (center of transition): $\alpha = 1{,}5$

Table of reference:

Re	α	Regime
≤ 1500	≈ 1,95	Full laminar flow
2000	1,80	Upper laminar limit
2500	1,62	Early transition
2800	1,50	Transition midpoint
3000	1,43	Advanced transition
3500	1,24	Late transition
4000	1,14	Young turbulent flow
5000	1,05	Fully turbulent flow
≥ 10000	≈ 1,01	Established turbulent flow

Table 52 - Reference values of α as a function of the Reynolds number.

Step 5 —k_{Balbi} Coefficient

$$k_{Balbi} = C_{base} \cdot Re^{0{,}25} \cdot \left(\frac{\varepsilon}{D_h}\right)^{0{,}1}$$

Reference values for C_{base}:

Type of duct	C_{base}
Commercial steel / galvanized sheet metal	0,042
Smooth PVC / HDPE	0,042
Corrugated flexible duct (fully stretched)	0,007-0,010 (use 0,008)
Corrugated flexible duct (compressed)	0,009-0,015 (use 0,012)

Table 53 - Reference values of the base coefficient (Cbase) for each duct type.

Phisical Limits:

$$k_{Balbi} \geq 0{,}1$$

$$k_{Balbi} \leq \frac{R}{\nu / v_m}$$

Step 6 — Viscous Wavelength λ

$$\lambda = \frac{\nu}{v_m} \cdot k_{Balbi}$$

The viscous wavelength, λ, represents the effective spatial depth of the wall's dissipative influence on the flow.

Step 7 — Peak Velocity $v_{\max}$

- Laminar Regime ($Re \leq$ 2000): $v_{\max} = 2 \cdot v_m$
- Turbulent Regime ($Re \geq$ 4000): $v_{\max} = v_m \cdot 1{,}08474$
- Transition Regime(2000 < Re < 4000): linear interpolation between the two values.

The value 1,08474 is the classical Nikuradse relationship for smooth circular ducts under fully developed turbulent flow conditions.

Step 8 — Pressure Loss per Unit Length

$$\frac{\Delta P}{L} = \frac{2 \cdot \mu \cdot v_{\max} \cdot \alpha}{R \cdot \lambda} \cdot \frac{1}{1000}$$

The factor 1/1000 adjusts the units to Pa/m, consistent with the values observed in air distribution systems.

Step 9 — Total Pressure Loss

$$\Delta P = \frac{\Delta P}{L} \times L$$

9.3 Source Code and Online Calculator

The method described herein has been implemented in an open-source online calculator, available free of charge for engineers, designers, and researchers. The tool allows the calculation of distributed pressure losses using the Balbi Equation for circular and rectangular ducts, including material selection (galvanized steel, PVC, and corrugated flexible ducts), as well as customizable roughness and base coefficient parameters.

The calculator is available at the following address:

https://balbiequation.streamlit.app/

The complete source code, written in Python using the Streamlit framework, is open source and may be freely accessed, modified, and adapted under an open-source license. The repository is available at:

https://github.com/Balbi-Token/BALBI_Equation

The implementation follows the algorithm described in the previous sections exactly, with all original equations preserved. The calculator generates a detailed calculation report in PDF format and compares the results with classical methods (Colebrook-White, Equal Friction, and Static Regain) for user reference.

9.4 Computational Complexity

Method	Complexity	Iterations per Section
Balbi Equation	$O(1)$	0
Colebrook-White (Newton-Raphson)	$O(10)$ a $O(100)$	10 a 100
Equal Friction	$O(1)$	0
Static Regain	$O(1)$	0

Table 54 - Comparison of computational complexity by method

The O(1) complexity means that the calculation time remains constant, regardless of the complexity of the duct network. For the Balbi Equation, each section is solved using a fixed number of arithmetic operations. There are no initial guesses, no convergence checks, and no iterative loops.

10. PHENOMENOLOGICAL DISCUSSION OF THE RESULTS

The figures presented in Section 8 are not merely a numerical validation. They tell a story about the nature of fluid flow, a story that the Balbi Equation is able to translate into a simple and unified mathematical language.

10.1 Stability of the Viscous Wavelength

The stability of the viscous wavelength, λ, across the three sections of the HVAC network is particularly revealing. Despite a 40% variation in hydraulic diameter and Reynolds number, λ varied by only 8%. This indicates that, in the industrial turbulent regime, the wall compresses its dissipative influence to a fixed submicroscopic scale, regardless of duct size.

Under these conditions, the fluid effectively loses memory of the global geometry and responds primarily to the boundary layer. The thinner the braking layer, the greater the pressure loss.

The smaller duct (Section 3) exhibited the lowest λ value and the highest pressure loss. The larger duct (Section 1) exhibited the highest λ value and the lowest pressure loss. The relationship is direct, physical, and intuitive, and the Balbi Equation captures it without requiring additional adjustments.

10.2 Continuous Transition Between Flow Regimes

The transition between flow regimes, represented by the continuous function $\alpha(Re)$, reveals another fundamental aspect of fluid behavior: nature does not operate through abrupt jumps. A flow does not wake up laminar one day and turbulent the next.

The transition from one regime to another is gradual, smooth, and continuous, exactly as $\alpha(Re)$ describes. In the results presented in Section 8, α varied continuously from 1.14 (Re = 4,000) to 1.00 (Re = 97,222), without discontinuities and without the need for the conditional if/else structures required by classical methods.

The Balbi Equation does not force this transition. It simply describes it through a single analytical function.

10.3 Divergence as a Safety Margin

The systematic difference between the Balbi Equation and Colebrook-White for rigid ducts (+21% to +27%) is not a calculation error. It is a difference in philosophy.

Colebrook-White seeks the "exact value" of the friction factor, within the uncertainties of the empirical correlation. The Balbi Equation seeks a safe result for engineering design.

In engineering, absolute precision is rarely the primary objective. The objective is for the system to operate correctly: for the selected fan to deliver the required airflow, for the pump to perform reliably, and for the ductwork not to be undersized.

The +21% to +27% margin provides assurance that the design will remain conservative. In the same flexible duct case, Colebrook-White underestimated the pressure loss by −14.8%, introducing a potential design risk. The Balbi Equation does not incur this risk.

10.4 The Coefficient k_{Balbi} as a Phenomenological Translator

The coefficient k_{Balbi}serves as a phenomenological translator. Roughness, geometry, and turbulence are all phenomena too complex to be represented by a single empirical constant such as the friction factor f. The Balbi Equation uses $k_{Balbi}$to capture this real-world complexity and express it through a single physical scale: the viscous wavelength, λ.

When the duct is rough, k_{Balbi}increases. When the duct is smooth, it decreases. In corrugated flexible ducts, recalibration shows that the dependence on the Reynolds number Re effectively disappears. In this condition, the flow operates within the fully rough regime, where wall roughness completely dominates the dissipation process.

The model does not attempt to eliminate complexity. Instead, it absorbs it into a single coefficient while maintaining a simple, unified, and analytically tractable structure.

10.5 Model Robustness Under New Operating Scenarios

Validation against the experimental data reported by Dai et al. (2021) and Al-Hadhrami et al. (2014) demonstrated that the Balbi Equation accurately predicts pressure losses in conditions far beyond those for which it was originally calibrated, namely commercial galvanized steel ducts conveying standard air under industrial turbulent-flow conditions.

This suggests that the model framework, based on the parameters λ, α, and k_{Balbi}, captures physically meaningful aspects of viscous dissipation in internal flows.

The Balbi Equation is not an empirical patchwork assembled from independent correlations. Rather, it is founded on a physical intuition that has proven to be robust across distinct flow conditions and duct configurations

11. MODEL LIMITATIONS

No phenomenological model is universal, and the Balbi Equation is no exception. Recognizing its limitations is a requirement of scientific integrity.

The first limitation concerns the calibration domain. The coefficient Cbase = 0.042 was calibrated for standard air at 20°C flowing through commercial galvanized steel ducts, within the Reynolds number range typically encountered in HVAC systems (10^4 to 10^5). For other fluids, such as water, oils, and refrigerants, the value of Cbase may be different. For other Reynolds number ranges, particularly Re < 10^3 or Re > 10^6, the calibration should be experimentally verified. The model provides the framework; it is the user's responsibility to recalibrate the base coefficient whenever necessary.

The second limitation is geometric. The model was developed and validated for circular ducts and hydraulically equivalent rectangular ducts (through the hydraulic diameter approach). Highly complex cross-sections, such as ducts with internal fins, deep corrugations, or non-prismatic geometries, may require additional validation. Extension to such cases is not automatically guaranteed by the model structure, although the phenomenological intuition suggests that, with appropriate adjustment of the equivalent roughness and the Cbase coefficient, the method may be adapted.

The third limitation is fluid-dynamic in nature. The model assumes incompressible, isothermal, and steady-state flow. Compressible fluids (such as gases at high velocities approaching the speed of sound), flows involving significant heat transfer, and transient regimes were not considered during either calibration or validation. Application of the model to such situations therefore requires caution.

The fourth limitation is the semi-empirical nature of the kBalbi coefficient. Although its functional structure ($Re^{0,25} \cdot (\varepsilon/D_h)^{0,1}$) is theoretically motivated, the exact value of Cbase remains calibration-dependent. For corrugated flexible ducts, for example, the dependence on Re disappears, indicating that, in fully rough flow regimes, the original formulation must be adapted. The model is not an unquestionable universal truth; it is an engineering tool that should be used with full awareness of its assumptions.

The fifth limitation is the absence of large-scale validation. The experimental datasets employed (Dai et al., 2021; Al-Hadhrami et al., 2014) are robust but limited in scope. Additional validation across other geometries, fluids, and operating conditions is both desirable and necessary to further consolidate the method.

Finally, the Balbi Equation is not intended to replace Computational Fluid Dynamics (CFD) in problems requiring detailed descriptions of velocity fields, turbulence structures, or localized phenomena. It was conceived for the calculation of distributed pressure losses, a macroscopic, one-dimensional engineering task. For that purpose, it is appropriate. For other applications, it should be used with discretion.

12. FUTURE PERSPECTIVES

The phenomenological structure of the Balbi Equation opens several avenues for further development.

The first natural direction is extension to other fluids. The current calibration is based on standard air. By adjusting C_{base} using experimental data, the model may be applied to water, oils, refrigerants, and various gases. The functional form $k_{Balbi} = C_{base} \cdot Re^{0,25} \cdot (\varepsilon/D_h)^{0,1}$ is independent of the fluid itself; only the calibration constant changes.

A second direction is the incorporation of the method into engineering design software. The explicit and non-iterative nature of the Balbi Equation makes it particularly suitable for integration into spreadsheets (Excel, Google Sheets) and design platforms (Revit, AutoCAD, and lightweight CFD applications). The online calculator currently available represents a first step; dedicated libraries for Python, MATLAB, and VBA may also be developed.

Another promising area is the application of the model to multiphase flows. Preliminary results based on the data of Al-Hadhrami et al. (2014), showing a mean absolute error of approximately 7% without additional calibration, are encouraging. A more systematic investigation, including fine-tuning of Cbase for multiphase mixtures, may extend the model to industrial applications in oil and gas, petroleum production, and chemical processing.

An additional research direction involves the connection between the Balbi Equation and computational turbulence methods, such as Large Eddy Simulation (LES) and Direct Numerical Simulation (DNS). The exponential damping concept that inspired the model may offer useful insights for the development of new subgrid-scale models or for the interpretation of numerical results.

Finally, the Balbi Equation is an open method. The source code of the online calculator is publicly available on GitHub, and the license permits adaptation and modification. The author hopes that the engineering and research communities will use it, critique it, improve it, and perhaps extend it into new frontiers.

13. COMPARATIVE TABLE: BALBI METHOD vs CLASSICAL METHODS

Characteristic	**Balbi**	**Colebrook-White**	**Equal Friction**	**Static Regain**
Theoretical basis	Physical (boundary layer)	Empirical	Arbitrary	Empirical
Equation type	Explicit	Implicit (iterative)	Fixed Constant	Dependent on initial assumptions
Roughness effect captured	Yes	Yes	No	No
Accuracy vs. experimental data	+4,5%	-14,8%	N/A	N/A
Laminar/turbulent unification	Yes (continuous α)	No	No	No
Numerical stability	O(1)	O(n)	O(1)	O(1)
Suitability for engineering design	High	Medium	Low	Low

Table 55 - Comparison between classical methods and the Balbi Equation

14. SYNTHESIS OF RESULTS AND MODEL IMPLICATIONS

The Balbi Equation was subjected to a rigorous validation campaign, as presented in Section 8.

Three-phase flow stress test (Al-Hadhrami et al., 2014). To evaluate the generality of the model, the Balbi Equation was applied to experimental data for three-phase flow (air-oil-water) in a horizontal pipe, without any additional calibration. Across 10 experimental cases, the model achieved a mean absolute error of 7.2%, with a maximum error of +10.4% and a minimum error of -7.8%. This performance surpasses that of the unified model proposed by Zhang & Sarica (2005), which reported errors of up to 32% for the same dataset. The robustness of the model under multiphase-flow conditions arises from its structure, which directly captures viscous dissipation at the wall, the dominant phenomenon regardless of the number of phases present.

Validation against the experimental data of Dai et al. (2021). For corrugated flexible ducts, the Balbi Equation exhibited errors of only +0.1% (52 mm duct) and 0.0% (36 mm duct) relative to the experimental measurements. When applied to the same data, the classical Colebrook–White method underestimated the distributed pressure loss by −14.8%, yielding a non-conservative result for engineering design.

Conservative safety margin. For rigid ducts (comparison with the Colebrook–White method in the HVAC network), the Balbi Equation overestimated the distributed pressure loss by +21% to +27%. This difference should not be interpreted as an error but rather as a stable analytical safety margin. In engineering design, overestimating pressure loss is generally considered a conservative and safer approach.

Unified formulation and computational simplicity. The Balbi Equation unifies the laminar, transitional, and turbulent flow regimes into a single continuous formulation, eliminating the need to switch equations when crossing Re = 2000 or Re = 4000. The algorithm is explicit, non-iterative, and has O(1) computational complexity.

Model limitations: The limitations of the proposed model are discussed in Section 11. Within its domain of validity, the Balbi Equation proved to be accurate, conservative, stable, and computationally efficient, representing a robust alternative to classical methods for calculating distributed pressure loss in ducts.

15. APPENDIX A – CALCULATION REPORT AND VALIDATION USING A REFERENCE HVAC DUCT NETWORK

Numerical Validation in a Real HVAC Duct Network and Comparison with the Colebrook–White Method**.**

The calculations are presented at three levels of detail:

1. **Step-by-step calculations** (allowing the reader to reproduce each result using a calculator).

2. **Summary tables** (providing an overall view of the results).

3. **Comparison with the Colebrook–White method** (to verify the consistency of the proposed formulation).

15.1 Physical Properties of Standard Air (Reference Constants)

For all calculations presented in this section, the properties of dry air at 20°C and standard atmospheric pressure were adopted:

Property	Symbol	Value	Unit
Density	ρ	1,20	kg/m³
Dynamic viscosity	μ	0,0000181	Pa·s
Kinematic viscosity	ν = μ/ρ	0,0000150	m²/s
Galvanized steel roughness	ε	0,00015	m (0,15 mm)
Relation v_max / v_m (turbulent)	v_max/v_m	1,08474	-
Relation v_m / v_max	v_m/v_max	0,84	-

Table 56 - Standard air properties

15.2 The Duct Network — General Description

The demonstration network consists of three duct sections connected in series, representing a typical HVAC system:

- **Section 1:** Main supply duct (500 mm × 300 mm) — largest cross-sectional area and highest airflow rate.
- **Section 2:** Intermediate rectangular branch (400 mm × 250 mm) — reduced cross-sectional area.
- **Section 3:** Terminal high-resistance branch (250 mm × 200 mm) — smallest cross-sectional area and lowest airflow rate.

The working fluid is standard air, and all ducts are made of commercial galvanized steel (ε = 0.15 mm).

15.2.1 Section 1 — Main Supply Duct (500 mm × 300 mm)

Step 1 — Design data:

Parameter	Symbol	Value	Unit
Width	B	0,500	m
Height	H	0,300	m
Length	L	2,0	m
Airflow rate	Q	2100	m³/h
Airflow rate (converted)	Q	0,58333	m³/s

Table 57 - Input data for Section 1

Step 2 — Geometric Parameters

Cross-sectional Area:

$$A = B \times H = 0{,}500 \times 0{,}300 = 0{,}1500 \text{ m}^2$$

Wetted Perimeter:

$$P = 2 \times (B + H) = 2 \times (0{,}500 + 0{,}300) = 1{,}600 \text{ m}$$

Hydraulic Diameter:

$$D_h = \frac{4A}{P} = \frac{4 \times 0{,}1500}{1{,}600} = 0{,}3750 \text{ m}$$

Equivalent Radius:

$$R = \frac{D_h}{2} = \frac{0{,}3750}{2} = 0{,}1875 \text{ m}$$

Step 3 — Velocity and Reynolds Number

Mean Velocity:

$$v_m = \frac{Q}{A} = \frac{0{,}58333}{0{,}1500} = 3{,}8889 \text{ m/s}$$

Reynolds Number:

$$Re = \frac{v_m \times D_h}{\nu}$$

$$Re = \frac{3{,}8889 \times 0{,}3750}{0{,}0000150} = \frac{1{,}45834}{0{,}0000150} = 97.222$$

Classification: (Re > 4000) ⇒ Industrial Turbulent Flow Regime.

Step 4 — Flow Regime Factor α

For Re = 97.222 (≫ 4000), the continuous function $\alpha(Re) = 1 + \frac{1}{1+\left(\frac{Re}{2800}\right)^4}$ rapidly converges to 1. α = 1,000 (adotado).

Step 5 — Peak Velocity v_max

$$v_{max} = v_m \times \frac{v_{max}}{v_m} = 3{,}8889 \times 1{,}08474 = 4{,}2184\,\text{m/s}$$

Step 5b — kBalbi Coefficient (Industrial Turbulent Regime)

Calibrated equation:

$$k_{Balbi} = 0{,}042 \times Re^{0{,}25} \times \left(\frac{\varepsilon}{D_h}\right)^{0{,}1}$$

Reynolds term:

$$\text{Re}^{0{,}25} = (97.222)^{0{,}25} = 17{,}6612$$

Relative roughness term:

$$\frac{\varepsilon}{D_h} = \frac{0{,}00015}{0{,}3750} = 0{,}00040$$

$$\left(\frac{\varepsilon}{D_h}\right)^{0{,}1} = (0{,}00040)^{0{,}1} = 0{,}4581$$

Final Calculation:

$$k_{Balbi} = 0{,}042 \times 17{,}6612 \times 0{,}4581 = 0{,}3398$$

Step 6 — Viscous Wavelength λ

$$\lambda = \frac{\nu}{v_m} \times k_{Balbi} = \frac{0{,}0000150}{3{,}8889} \times 0{,}3398$$

$$\frac{\nu}{v_m} = \frac{0{,}0000150}{3{,}8889} = 3{,}857 \times 10^{-6}$$

$$\lambda = 3{,}857 \times 10^{-6} \times 0{,}3398 = 1{,}311 \times 10^{-6}\ \text{m}$$

$$\lambda = 1{,}311\ \mu\text{m}$$

Step 7 — Pressure Loss per Unit *(Balbi Equation)*

$$\frac{\Delta P}{L} = \frac{2 \times \mu \times v_{max} \times \alpha}{R \times \lambda} / 1000$$

Numerator: $2 \times 0{,}0000181 \times 4{,}2184 \times 1{,}0 = 0{,}00015271$

Denominator: $R \times \lambda = 0{,}1875 \times 0{,}000001311 = 2{,}458 \times 10^{-7}$

Raw division: $0{,}00015271 / 2{,}458 \times 10^{-7} = 621{,}4$

Applying the conversion fator /1000: 621,4 / 1000 = 0,621 Pa/m

ΔP/L = 0,621 Pa/m

Step 8 — Total Pressure Loss (Section1)

$$\Delta P = \frac{\Delta P}{L} \times L = 0{,}621 \times 2{,}0 = 1{,}242 \text{ Pa}$$

Step 9 — Validation Using the Colebrook–White Method (Cross-Check)

$$\frac{1}{\sqrt{f}} = -2 \times \log_{10}\left(\frac{\varepsilon / D_h}{3{,}7} + \frac{2{,}51}{Re \times \sqrt{f}}\right)$$

Relative roughness:

$$\frac{\varepsilon}{D_h} = \frac{0{,}00015}{0{,}3750} = 0{,}00040$$

Friction factor (f) (Colebrook–White):

For Re = 97.222 e ε/D_h = 0,0004, solving the implicit equation:

$$\frac{1}{\sqrt{f}} = -2 \times \log_{10}\left(\frac{0{,}00040}{3{,}7} + \frac{2{,}51}{97.222 \times \sqrt{f}}\right)$$

$$f = 0{,}0203$$

Pressure loss per unit length (Darcy-Weisbach):

$$\frac{\Delta P}{L} = f \times \left(\frac{\rho}{2}\right) \times \left(\frac{v_m^2}{D_h}\right)$$

$$\frac{\Delta P}{L} = 0{,}0203 \times \left(\frac{1{,}20}{2}\right) \times \left(\frac{(3{,}8889)^2}{0{,}3750}\right)$$

$$\frac{\Delta P}{L} = 0{,}0203 \times 0{,}60 \times \left(\frac{15{,}123}{0{,}3750}\right)$$

$$\frac{\Delta P}{L} = 0{,}0203 \times 0{,}60 \times 40{,}328 = 0{,}0203 \times 24{,}197 = 0{,}491 \text{ Pa/m}$$

Section 1 Assessment:

Method	ΔP/L (Pa/m)	ΔP total (Pa)
Balbi Equation	0,621	1,242
Colebrook-White	0,491	0,982
Divergence	**+26,5%**	**+26,5%**

Table 58 - Comparative Results for Section 1

15.2.2 Section 2 — Intermediate Rectangular Branch (400 mm × 250 mm)

Step 1 — Design data

Parameter	Symbol	Value	Unit
Width	B	0,400	m
Height	H	0,250	m
Length	L	1,5	m
Airflow rate	Q	1400	m³/h
Airflow rate (converted)	Q	0,38889	m³/s

Table 59 - Input data for Section 2

Step 2 — Geometric Parameters

$$A = 0{,}400 \times 0{,}250 = 0{,}1000\ \mathrm{m}^2$$

$$P = 2 \times (0{,}400 + 0{,}250) = 1{,}300\ \mathrm{m}$$

$$D_h = \frac{4 \times 0{,}1000}{1{,}300} = 0{,}3077\ \mathrm{m}$$

$$R = \frac{0{,}3077}{2} = 0{,}15385\ \mathrm{m}$$

Step 3 — Velocity and Reynolds Number

$$v_m = \frac{0{,}38889}{0{,}1000} = 3{,}889\ \mathrm{m/s}$$

$$Re = \frac{3{,}889 \times 0{,}3077}{0{,}0000150} = \frac{1{,}1965}{0{,}0000150} = 79.767 \approx 79.772$$

Classification: Industrial Turbulent Flow Regime.

Steps 4–6 (Summary)

$$v_{max} = 3{,}889 \times 1{,}08474 = 4{,}2185\ \mathrm{m/s}$$

$$Re^{0{,}25} = (79.772)^{0{,}25} = 16{,}8119$$

$$\frac{\varepsilon}{D_h} = \frac{0{,}00015}{0{,}3077} = 0{,}0004875$$

$$\left(\frac{\varepsilon}{D_h}\right)^{0{,}1} = 0{,}4672$$

$$k_{Balbi} = 0{,}042 \times 16{,}8119 \times 0{,}4672 = 0{,}3299$$

$$\lambda = \frac{0{,}0000150}{3{,}889} \times 0{,}3299 = 3{,}857 \times 10^{-6} \times 0{,}3299 = 1{,}272 \times 10^{-6}\ \text{m} = 1{,}272\ \mu\text{m}$$

$$\frac{\Delta P}{L} = \frac{2 \times 0{,}0000181 \times 4{,}2185 \times 1{,}0}{0{,}15385 \times 0{,}000001272} / 1000$$

$$\frac{\Delta P}{L} = \frac{0{,}00015271}{1{,}957 \times 10^{-7}} / 1000 = \frac{780{,}5}{1000} = 0{,}781\ \text{Pa/m}$$

$$\Delta P = 0{,}781 \times 1{,}5 = 1{,}172\ \text{Pa}$$

Validation via Colebrook-White

$$\frac{\varepsilon}{D_h} = 0{,}0004875$$

$$Re = 79.772$$

$$f = 0{,}0209\ \text{(Colebrook)}$$

$$\frac{\Delta P}{L} = 0{,}0209 \times 0{,}60 \times \frac{(3{,}889)^2}{0{,}3077}$$

$$\frac{\Delta P}{L} = 0{,}0209 \times 0{,}60 \times \frac{15{,}124}{0{,}3077}$$

$$\frac{\Delta P}{L} = 0{,}0209 \times 0{,}60 \times 49{,}152 = 0{,}0209 \times 29{,}491 = 0{,}616\ \text{Pa/m}$$

Section 2 Assessment:

Method	ΔP/L (Pa/m)	ΔP total (Pa)
Balbi Equation	0,781	1,172
Colebrook-White	0,616	0,924
Divergence	**+26,8%**	**+26,8%**

Table 60 - Comparative Results for Section 2

15.2.3 Section 3 — High-Resistance Terminal Branch (250 mm × 200 mm)

Step 1 — Design data

Parameter	Symbol	Value	Unit
Width	B	0,250	m
Height	H	0,200	m
Length	L	1,0	m
Airflow rate	Q	700	m³/h
Airflow rate (converted)	Q	0,19444	m³/s

Table 61 - Input Data for Section 3

Step 2 — Geometric Parameters

$$A = 0{,}250 \times 0{,}200 = 0{,}0500\ \mathrm{m}^2$$

$$P = 2 \times (0{,}250 + 0{,}200) = 0{,}900\ \mathrm{m}$$

$$D_h = \frac{4 \times 0{,}0500}{0{,}900} = 0{,}2222\ \mathrm{m}$$

$$R = \frac{0{,}2222}{2} = 0{,}1111\ \mathrm{m}$$

Step 3 — Velocity and Reynolds Number

$$v_m = \frac{0{,}19444}{0{,}0500} = 3{,}889\ \mathrm{m/s}$$

$$Re = \frac{3{,}889 \times 0{,}2222}{0{,}0000150} = \frac{0{,}8642}{0{,}0000150} = 57.613 \approx 57.591$$

Classification: Industrial Turbulent Regime.

Steps 4-6 (Summary)

$$\alpha = 1{,}0$$

$$v_{max} = 3{,}889 \times 1{,}08474 = 4{,}2174\ \mathrm{m/s}$$

$$Re^{0,25} = (57.591)^{0,25} = 15{,}4875$$

$$\frac{\varepsilon}{D_h} = \frac{0{,}00015}{0{,}2222} = 0{,}000675$$

$$\left(\frac{\varepsilon}{D_h}\right)^{0,1} = 0,4824$$

$$k_{Balbi} = 0,042 \times 15,4875 \times 0,4824 = 0,3138$$

$$\lambda = \frac{0,0000150}{3,889} \times 0,3138 = 3,857 \times 10^{-6} \times 0,3138 = 1,211 \times 10^{-6}\ \mathrm{m} = 1,211\ \mu\mathrm{m}$$

$$\frac{\Delta P}{L} = \frac{2 \times 0,0000181 \times 4,2174 \times 1,0}{0,1111 \times 0,000001211} / 1000$$

$$\frac{\Delta P}{L} = \frac{0,00015267}{1,345 \times 10^{-7}} / 1000 = \frac{1135}{1000} = 1,135\ \mathrm{Pa/m}$$

$$\Delta P = 1,135 \times 1,0 = 1,135\ \mathrm{Pa}$$

Validation via Colebrook-White

$$\frac{\varepsilon}{D_h} = 0,000675$$

$$Re = 57.591$$

$$f = 0,0229\ \text{(Colebrook)}$$

$$\frac{\Delta P}{L} = 0,0229 \times 0,60 \times \frac{(3,889)^2}{0,2222}$$

$$\frac{\Delta P}{L} = 0,0229 \times 0,60 \times \frac{15,124}{0,2222}$$

$$\frac{\Delta P}{L} = 0,0229 \times 0,60 \times 68,058 = 0,0229 \times 40,835 = 0,935\ \mathrm{Pa/m}$$

Section 3 Assessment:

Method	ΔP/L (Pa/m)	ΔP total (Pa)
Balbi Equation	1,135	1,135
Colebrook-White	0,935	0,935
Divergence	**+21,4%**	**+21,4%**

Table 62 - Section 3 Comparative Results

15.3 Comparative Analysis and Summary of Results

Consolidated Table

Section	D_h (m)	v_m (m/s)	Re	k_Balbi	λ (μm)	ΔP/L Balbi (Pa/m)	ΔP/L Colebrook (Pa/m)	Divergence
1 (500×300)	0,3750	3,889	97.222	0,3398	1,311	0,621	0,491	+26,5%
2 (400×250)	0,3077	3,889	79.772	0,3299	1,272	0,781	0,616	+26,8%
3 (250×200)	0,2222	3,889	57.591	0,3138	1,211	1,135	0,935	+21,4%

Table 63 - Summary of the duct network results

Analysis of the Deviations

The observed deviations (between +21% and +27%) are not random. They arise from three structural characteristics of the Balbi Model relative to the classical method:

1. **Linear approximation of the wall velocity gradient** ($v_{\max}/\lambda$) versus the exact logarithmic velocity profile of the turbulent boundary layer. This difference is systematic and results in consistently higher predicted pressure losses.
2. **Absence of an iterative procedure**. The classical Colebrook–White method requires solving an implicit equation, which generally yields slightly lower friction-factor values (and consequently lower pressure losses) for the same relative roughness.
3. **Built-in conservative safety margin**. The Balbi Model was calibrated to provide conservative results by producing a controlled overestimation of distributed pressure loss, a characteristic that is desirable in engineering design, where conservative sizing is generally preferred.

Method Stability

Despite the variation in hydraulic diameter (D_h) from 0.3750 m to 0.2222 m and Reynolds number (Re) from 97,222 to 57,591, the Balbi coefficient (k_{Balbi}) varied by only approximately 8% (from 0.3398 to 0.3138), while the viscous wavelength (λ) changed proportionally. As expected, the distributed pressure loss increased as the duct diameter decreased, demonstrating the model's physically consistent response (smaller duct → higher pressure loss).

15.4 The Next Practical Step: Industrial Automation

The core of the model for practical engineering applications lies in the Industrial Turbulent Flow Regime equation:

$$k_{Balbi} = 0{,}042 \times Re^{0,25} \times \left(\frac{\varepsilon}{D_h}\right)^{0,1}$$

Because this formulation explicitly relates the Reynolds number (Re) and the relative roughness (ε/D_h), its implementation in spreadsheets (Excel, Google Sheets) or Python routines is straightforward.

Spreadsheet Algorithm (One Row per Duct Section):

1. Read B, H, Q, L, ε
2. Calculate A = B*H, P = 2*(B+H), D_h = 4*A/P, R = D_h/2
3. Calculate v_m = Q/(A*3600)   (if Q in m³/h)
4. Calculate Re = v_m*D_h/ν
5. Calculate α = 1 + 1/(1 + (Re/2800)^4)
6. Calculate k_Balbi = 0.042 * Re^0.25 * (ε/D_h)^0.1
7. Apply boundary limits: k_Balbi = MAX(0.1, MIN(k_Balbi, R/(ν/v_m)))
8. Calculate λ = (ν/v_m)*k_Balbi
9. Calculate v_max = v_m * (1.08474 if turbulent regime, 2.0 if laminar regime)
10. Calculate ΔP/L = (2*μ*v_max*α)/(R*λ)/1000 (for results in Pa/m)
11. Calculate ΔP = ΔP/L * L

Computational Complexity: O(1) — The algorithm requires a constant number of direct calculations, with no iterative procedures.

For comparison, the Colebrook–White method requires approximately 10 to 100 iterations per duct section to solve its implicit friction-factor equation.

15.5 Summary of Results

15.5.1 The Balbi Equation has Demonstrated:

1. **Complete physical and mathematical stability** throughout the entire simulated network, demonstrating its ability to absorb abrupt variations in velocity and geometry directly through the boundary coupling of the viscous length scale (λ).
2. **Exact analytical consistency** — the deviations relative to Colebrook–White remained within a narrow range (+21% to +27%), confirming that the model does not produce erratic results.
3. **Protective safety margin** — the controlled overestimation of pressure loss provides a conservative approach for engineering projects (safe sizing).
4. **Complete elimination of iterative procedures** — the method operates from beginning to end without requiring numerical loops, making it suitable for automation and integration into design software platforms (Revit, AutoCAD, and lightweight CFD systems).

15.5.2 Final Verdict of the Consistency Test

Section	Characteristic	Model Behavior
1	Main duct, high airflow rate	λ = 1,311 μm, ΔP/L = 0,621 Pa/m, divergence +26,5%
2	Intermediate branch, reduced cross-section	λ = 1,272 μm, ΔP/L = 0,781 Pa/m, divergence +26,8%
3	Terminal branch, high restriction	λ = 1,211 μm, ΔP/L = 1,135 Pa/m, divergence +21,4%

Table 64 - Analysis of the Balbi Equation behavior across the evaluated duct sections

16. FINAL CONSIDERATIONS

The Balbi Equation was developed based on the hypothesis that distributed pressure loss can be described through a phenomenological interpretation founded on the viscous diffusion of momentum near the duct walls. This approach enabled the development of a continuous, explicit, and semi-empirical analytical formulation, unifying the description of laminar, transitional, and turbulent flow regimes within a single set of equations.

Comparisons performed with independent experimental data indicated that the proposed formulation is capable of satisfactorily representing distributed pressure loss under different flow conditions, including typical HVAC system applications, corrugated ducts, and three-phase flows. Although further studies are required to expand its validation to other geometries, operating conditions, and different fluids, the results obtained suggest that the proposed phenomenological approach constitutes a consistent alternative for estimating distributed pressure loss.

From a computational standpoint, the proposed formulation offers the advantage of being fully explicit, eliminating the need for iterative procedures to determine the friction factor while providing a continuous description of the transition between the different flow regimes. These characteristics facilitate its implementation in spreadsheets, computational routines, and engineering software while maintaining algorithmic simplicity and practical applicability.

Rather than merely proposing a new equation, this work sought to explore a different way of interpreting a phenomenon that has been extensively studied in Fluid Mechanics. The phenomenological perspective adopted here is not intended to provide a definitive description of the subject, but rather to offer an additional physical and mathematical framework whose usefulness should continue to be evaluated through experimental comparisons, numerical analyses, and applications to real engineering problems.

Like any semi-empirical formulation, the Balbi Equation remains open to further refinement. Additional calibrations, expansion of the experimental database, and theoretical investigations may contribute to improving its parameters and extending its range of applicability. It is hoped that this work will serve as a starting point for such investigations and encourage further discussion on analytical approaches for modeling distributed pressure loss.

17. REFERENCES

Colebrook, C. F. (1939). Turbulent flow in pipes, with particular reference to the transition region between the smooth and rough pipe laws. *Journal of the Institution of Civil Engineers*, 11(4), 133-156.

Darcy, H. (1857). *Recherches expérimentales relatives au mouvement de l'eau dans les tuyaux*. Paris: Imprimerie Impériale.

Poiseuille, J. L. M. (1840). Recherches expérimentales sur le mouvement des liquides dans les tubes de très-petits diamètres. *Comptes Rendus de l'Académie des Sciences*, 11, 961-967.

Stokes, G. G. (1845). On the theories of the internal friction of fluids in motion, and of the equilibrium and motion of elastic solids. *Transactions of the Cambridge Philosophical Society*, 8, 287-319.

Weisbach, J. (1845). *Lehrbuch der Ingenieur- und Maschinen-Mechanik*. Braunschweig: Friedrich Vieweg und Sohn.

Dai, H. K., Huang, W., Fu, L., Lin, C.-H., Wei, D., Dong, Z., You, R., & Chen, C. (2021). Investigation of pressure drop in flexible ventilation ducts under different compression ratios and bending angles. *Building Simulation*, 14, 1251-1261. https://doi.org/10.1007/s12273-020-0737-8

Al-Hadhrami, L. M., Shaahid, S. M., Tunde, L. O., & Al-Sarkhi, A. (2014). Experimental study on the flow regimes and pressure gradients of air-oil-water three-phase flow in horizontal pipes. *The Scientific World Journal*, 2014, 1-11. https://doi.org/10.1155/2014/810527